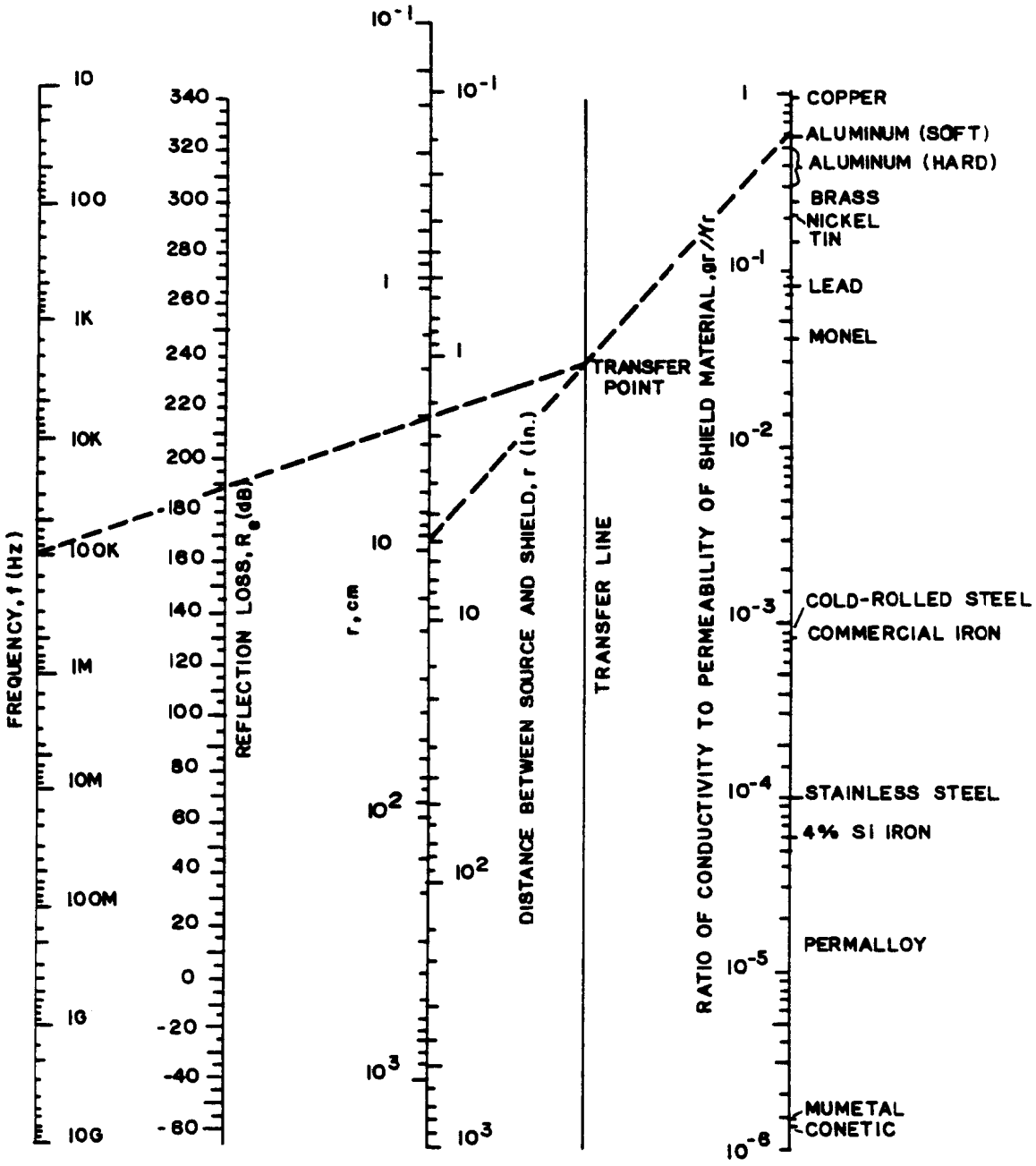

Figure 5-5. Nomograph for determining electric field reflection loss. (Source: ref 5-3)

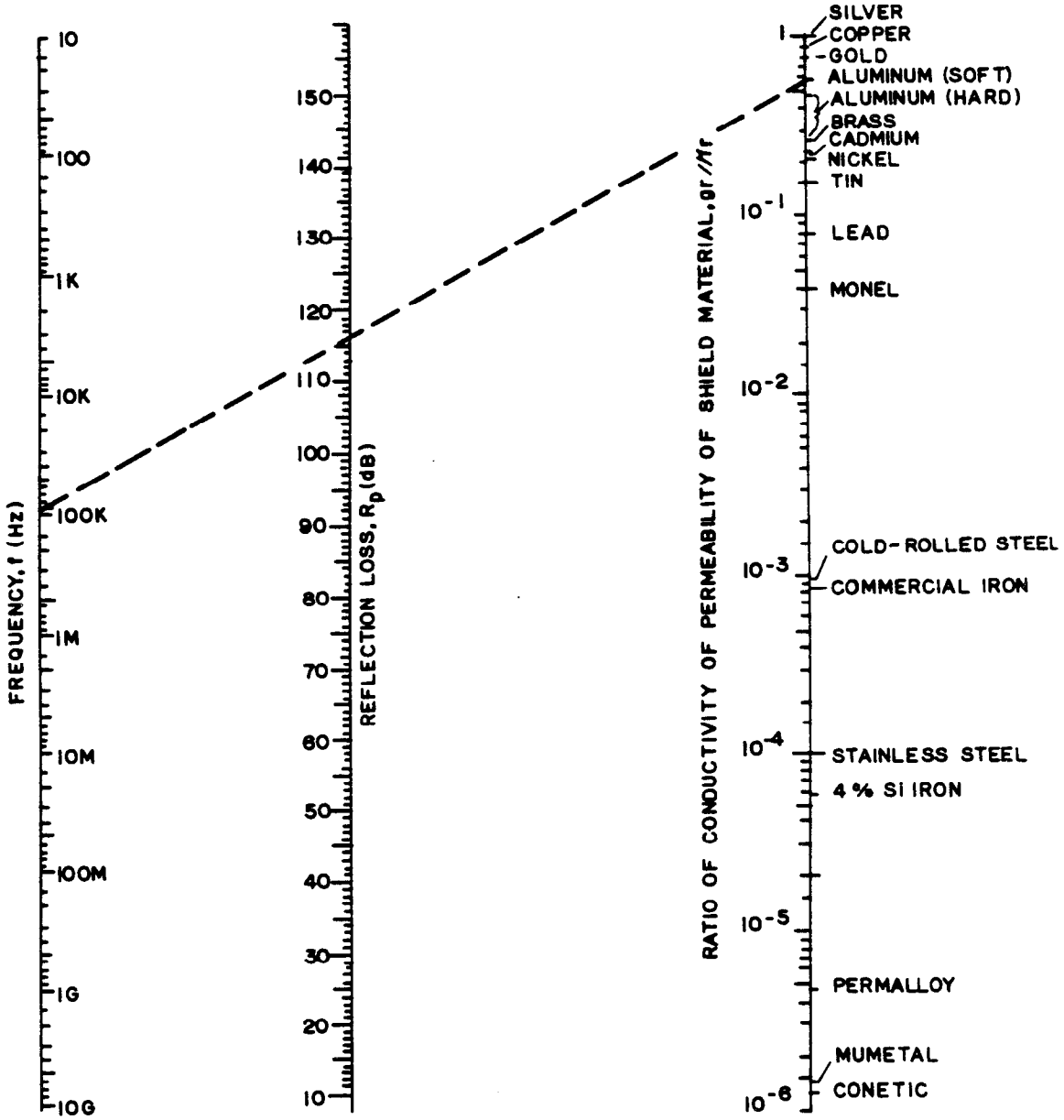

Figure 5-6. Nomograph for determining plane wave reflection loss. (Source: ref 5-3)

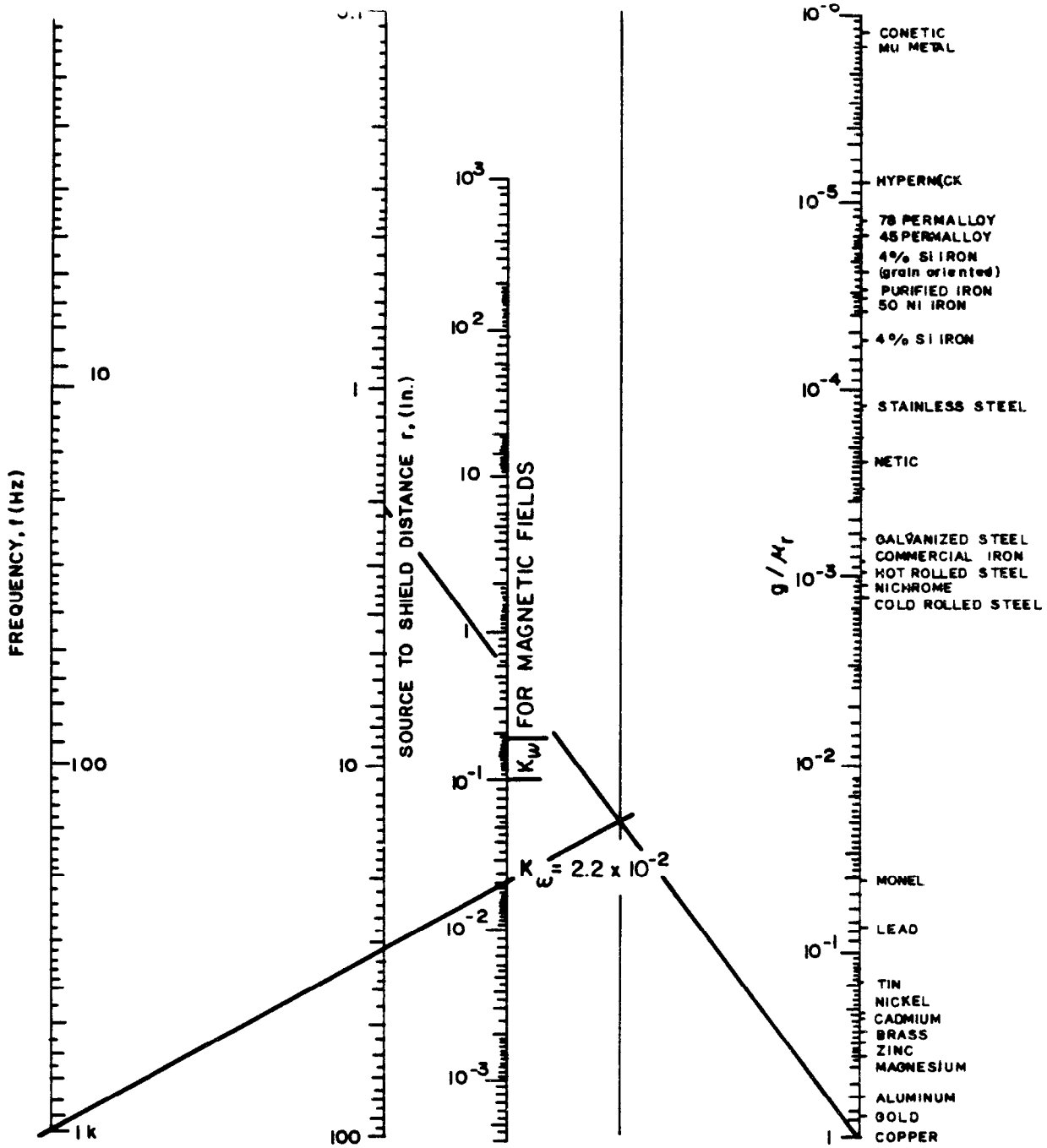

Figure 5-7. Chart for computing K for magnetic field secondary reflection loss. (Source: ref 5-3)

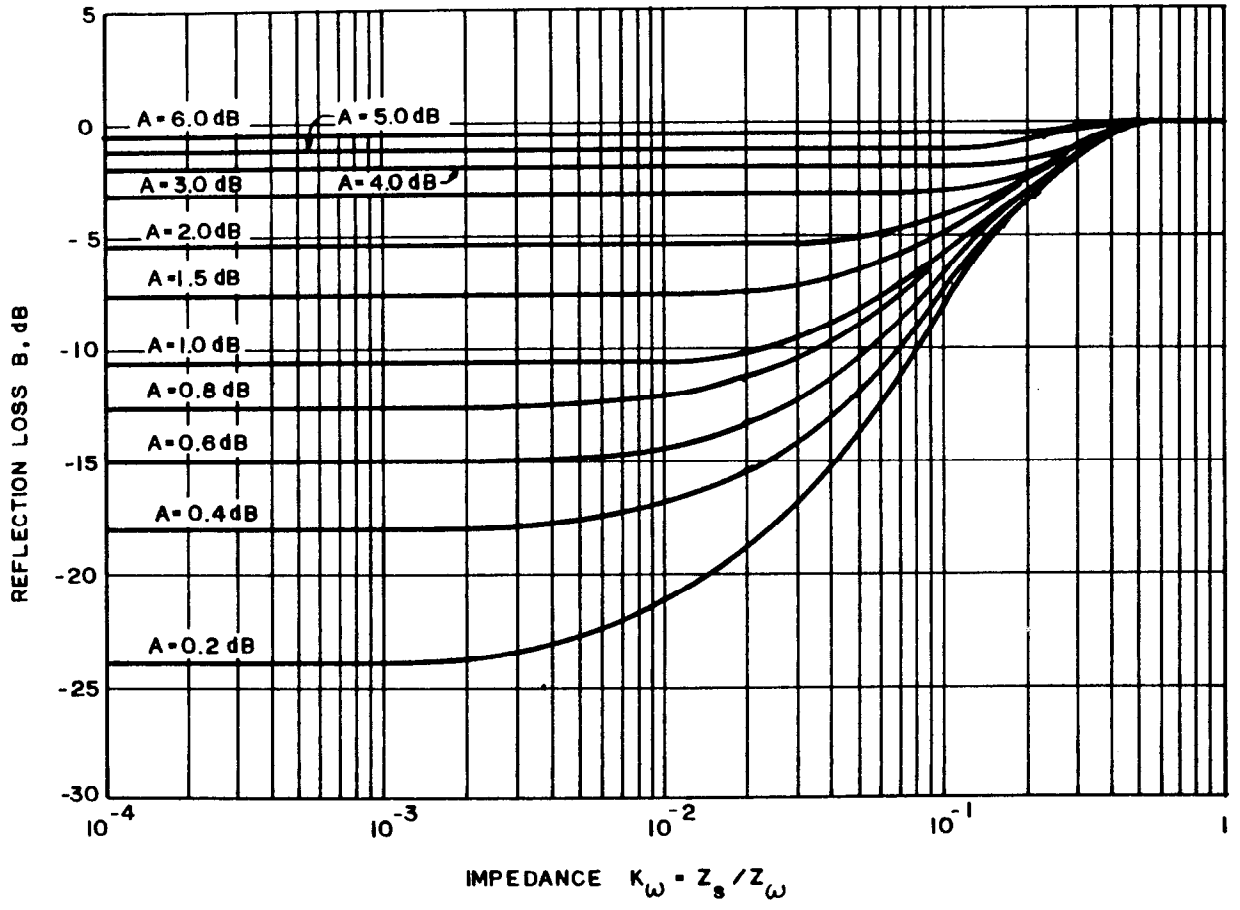

Figure 5-8. Chart for computing secondary losses for magnetic fields. (Source: ref 5-3)

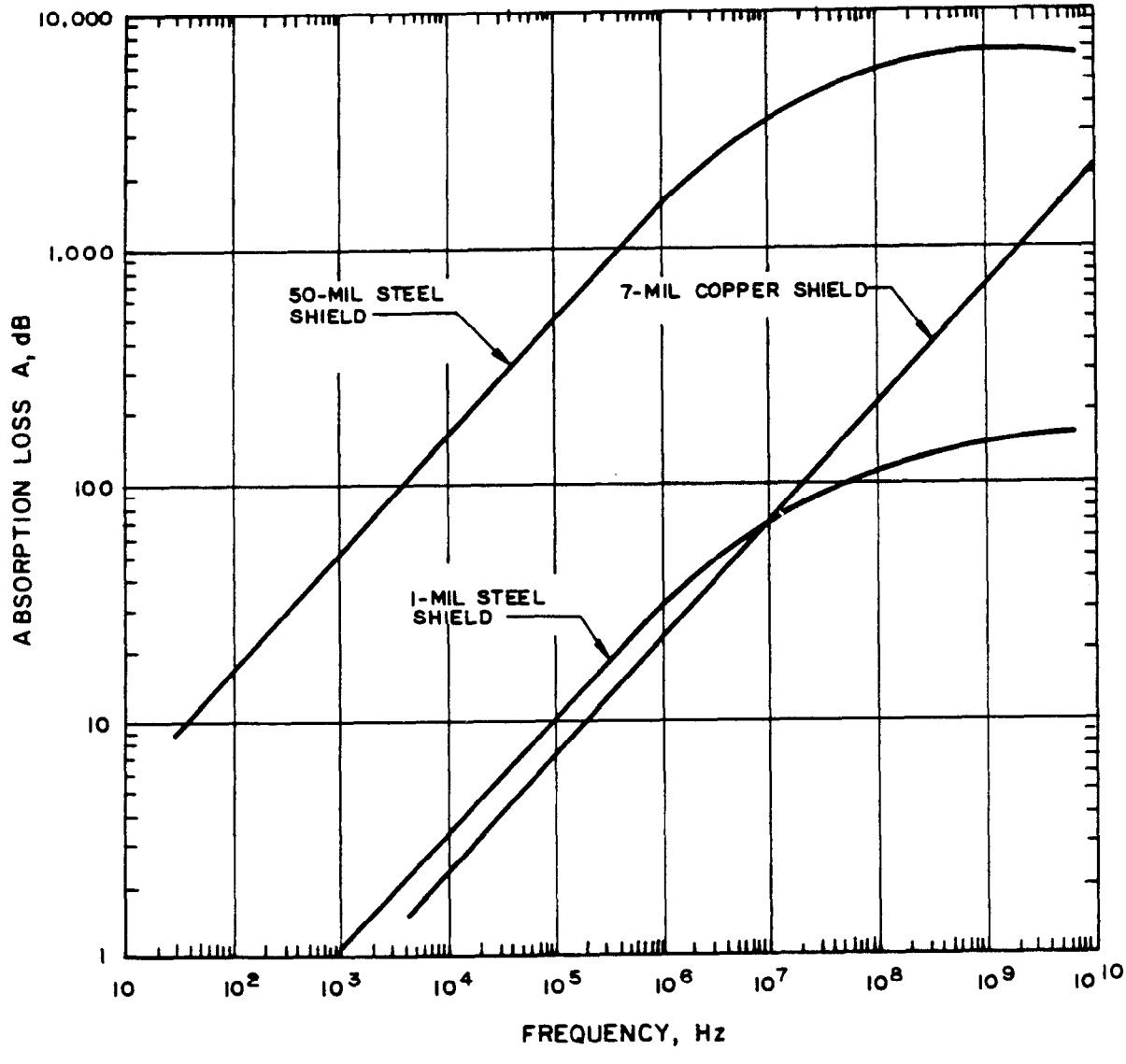

Figure 5-9. Absorption loss for steel and copper shields at 30 hertz to 10,000 megahertz. (Source: ref 5-3)

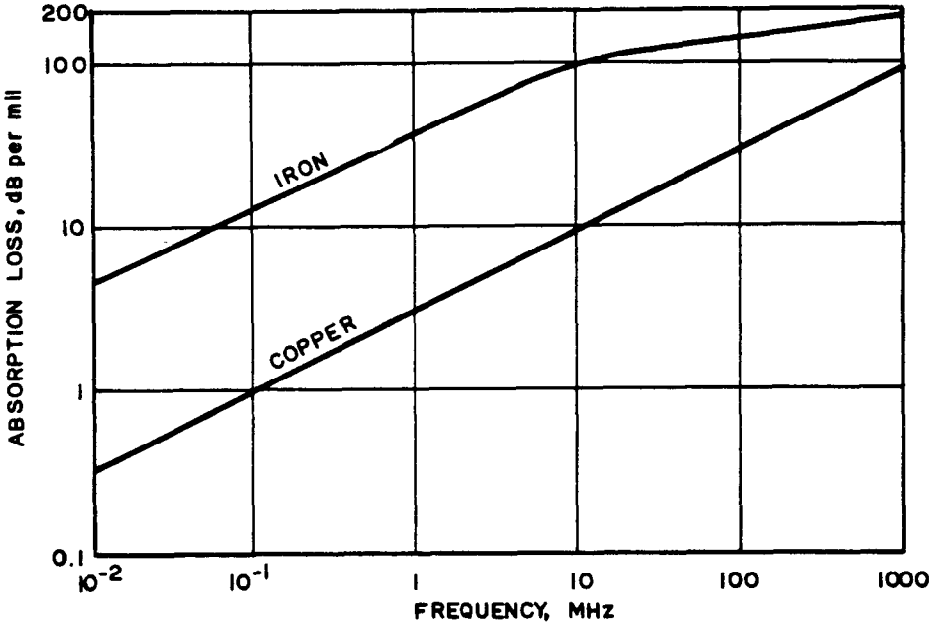

Figure 5-10. Absorption loss for copper and iron, in decibels per mil. (Source: ref 5-3)

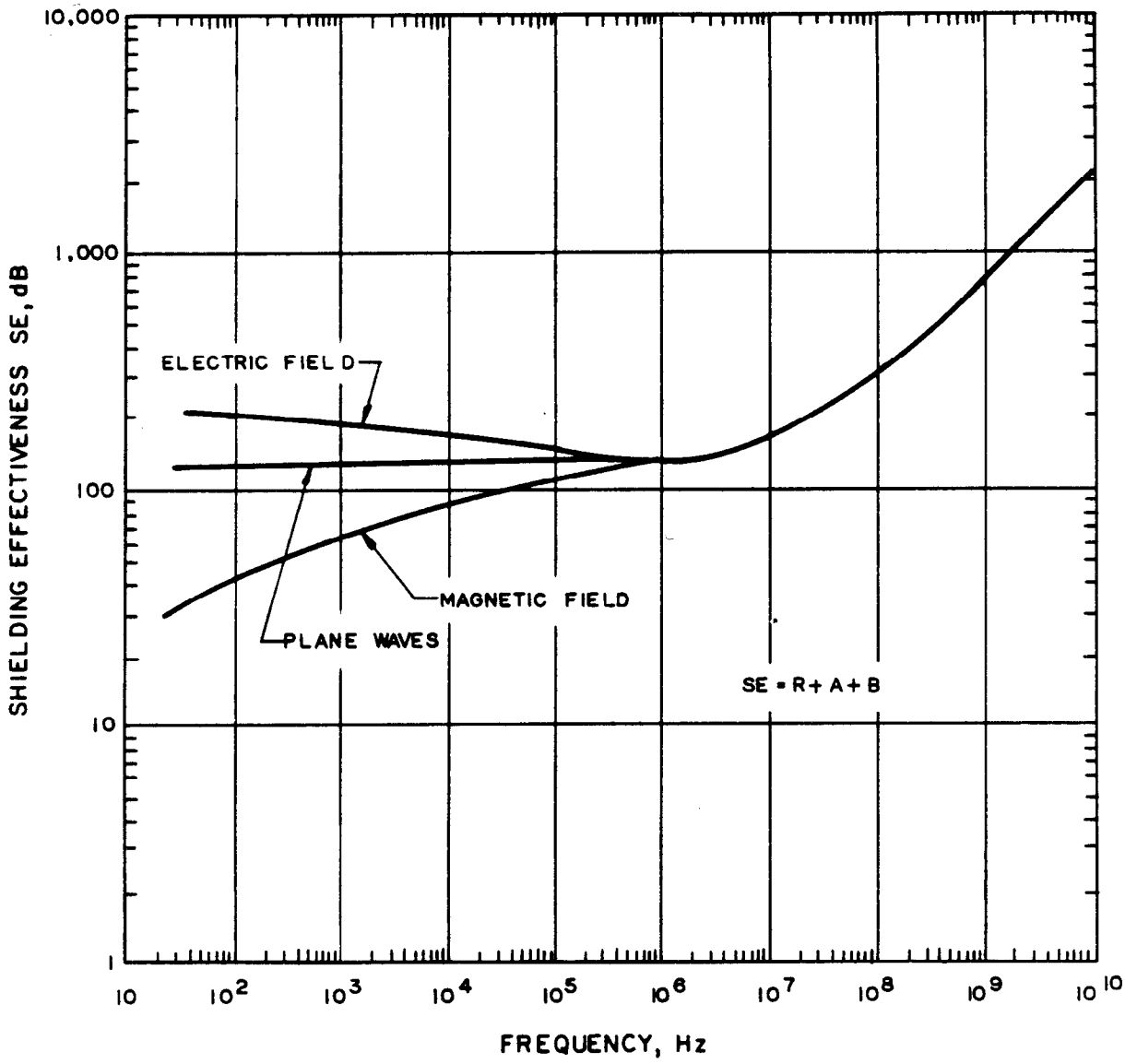

Figure 5-11. Shielding effectiveness in electric, magnetic, and plane wave fields of copper shields (7 mils thick) for signal source 165 feet from the shield. (Source: ref 5-3)

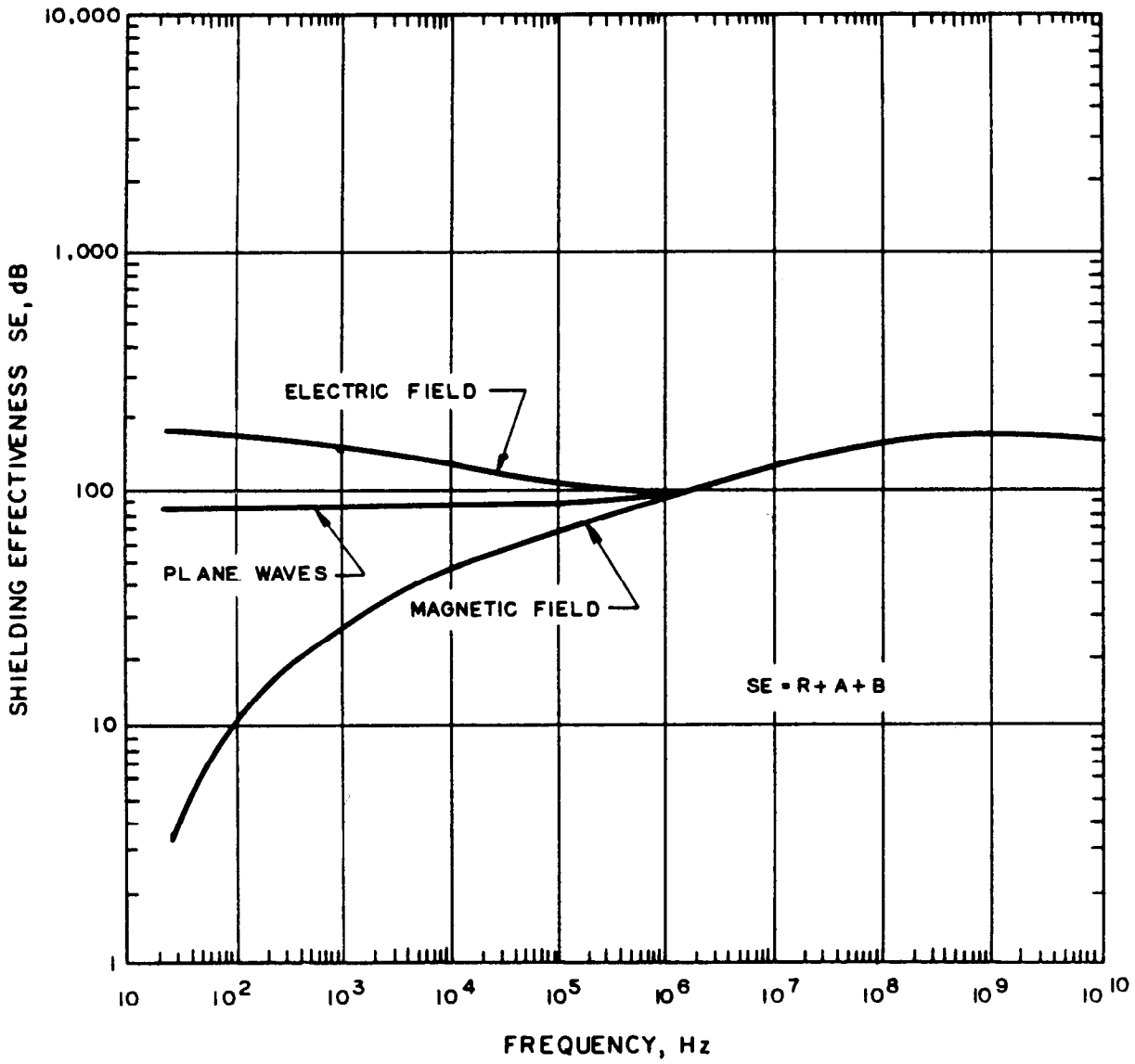

Figure 5-12. Shielding effectiveness in electric, magnetic, and plane wave fields of steel shield (1 mil thick) for signal sources 165 feet from the shield. (Source: ref 5-3)

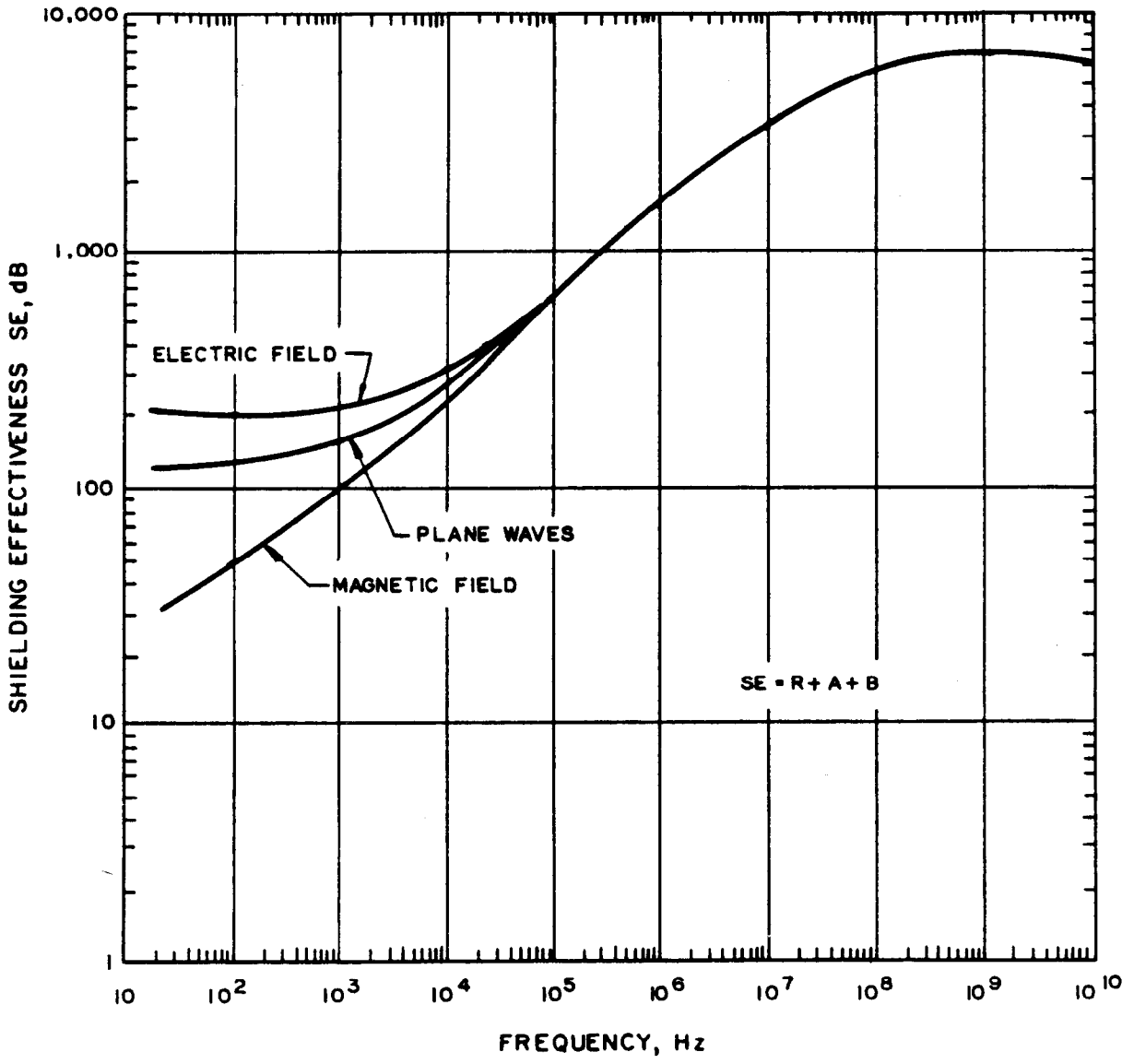

Figure 5-13. Shielding effectiveness in electric, magnetic, and plane wave fields of steel shield (50 mils thick) for signal sources 165 feet from the shield. (Source: ref 5-3)

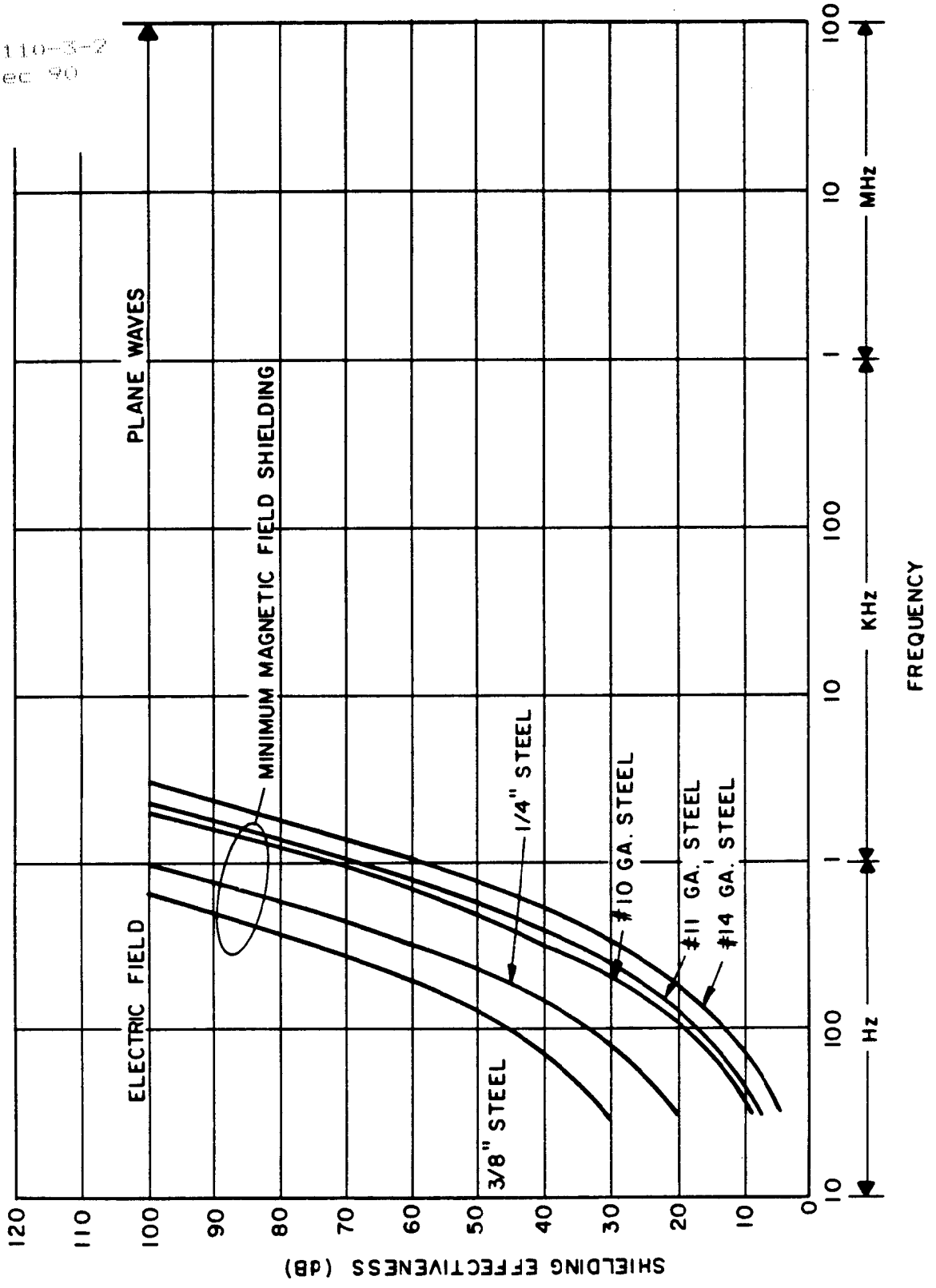

Figure 5-14. Minimum shielding effectiveness of low-carbon steel walls. (Source: ref 5-28)

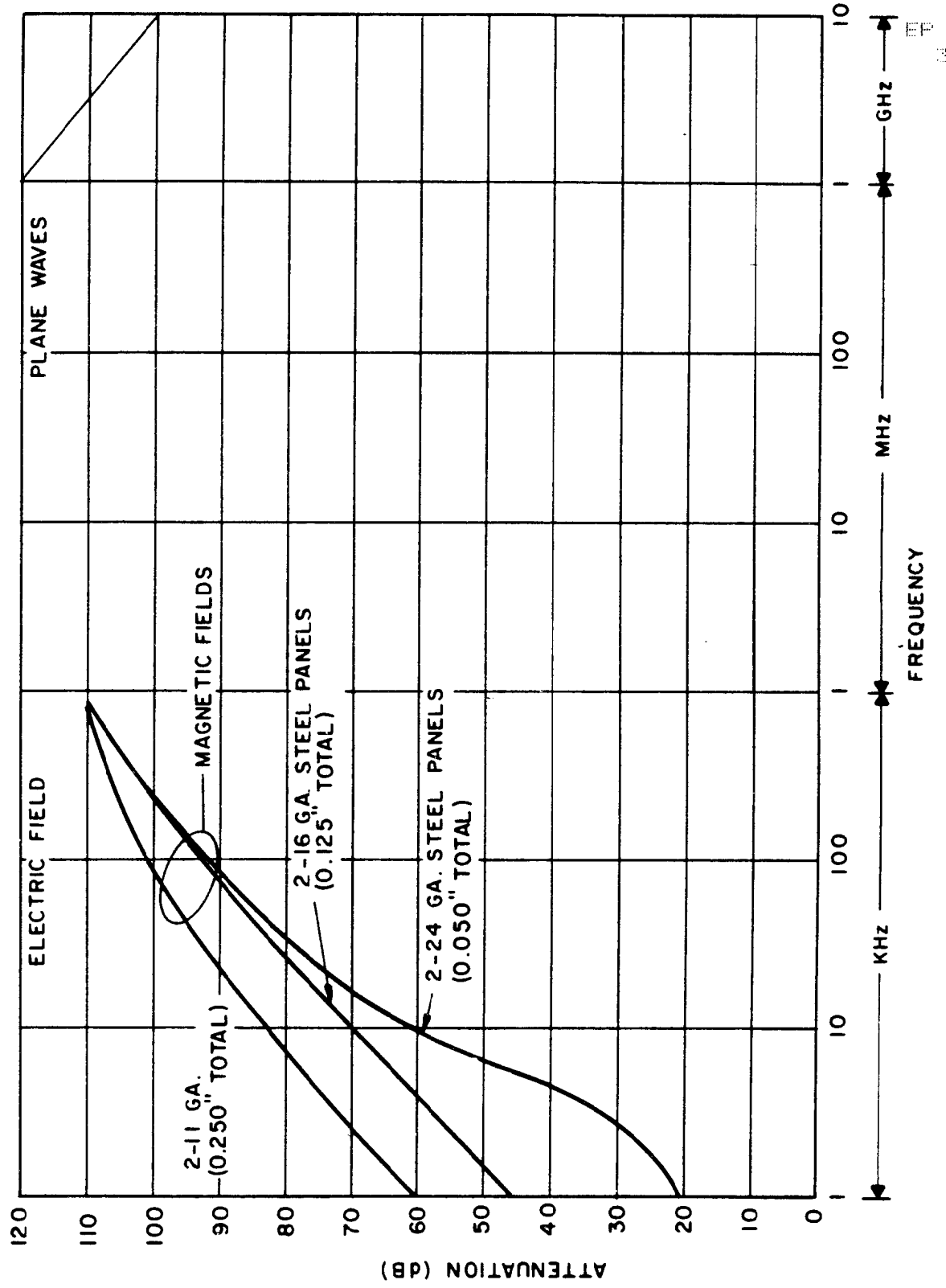

Figure 5-15. Performance characteristics of typical commercial shielded enclosures. (Source: ref 5-28)

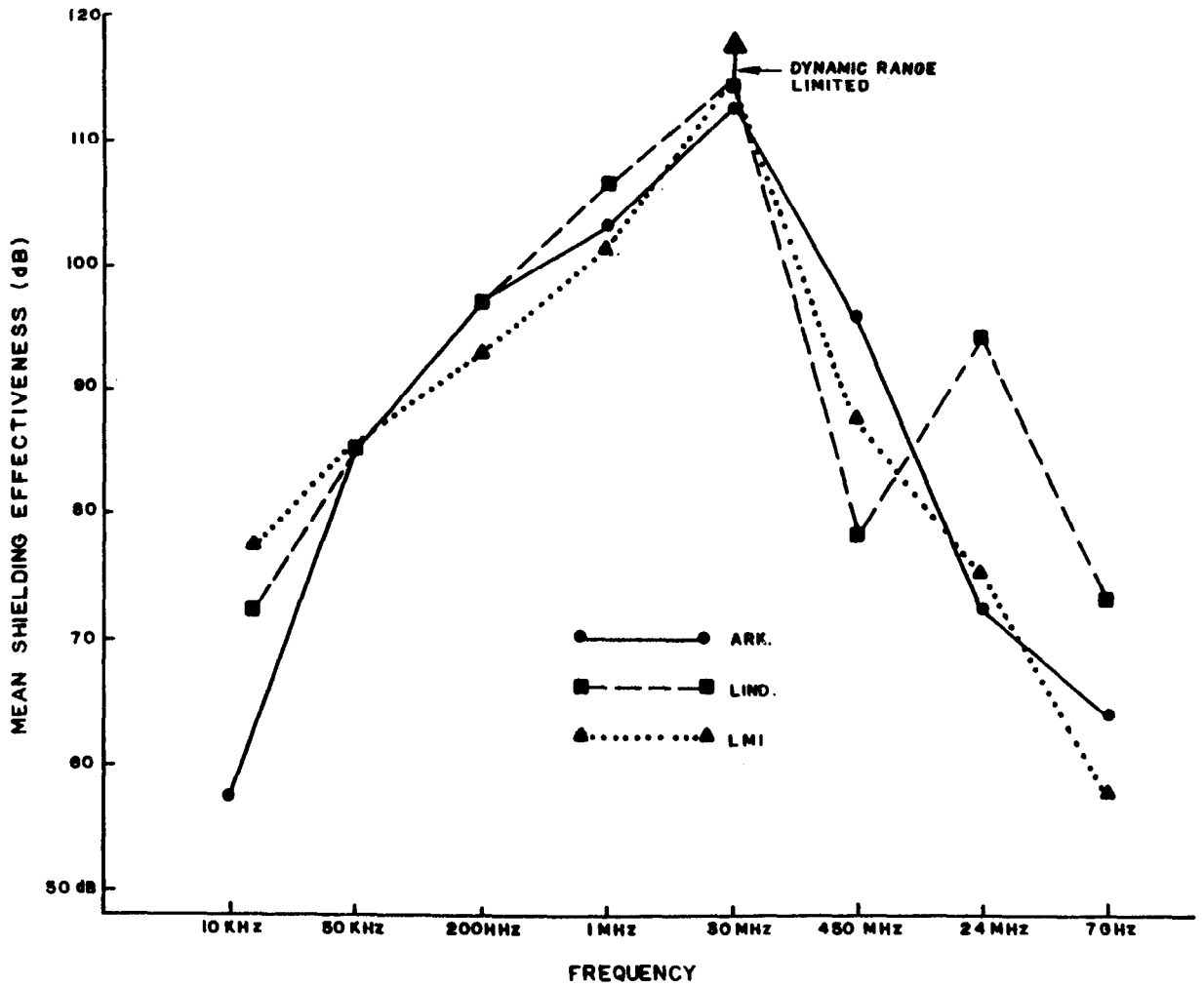

Figure 5-16. Mean shielding effectiveness for all test points for the June 1980 test. (Source: ref 5-29)

This page not used.

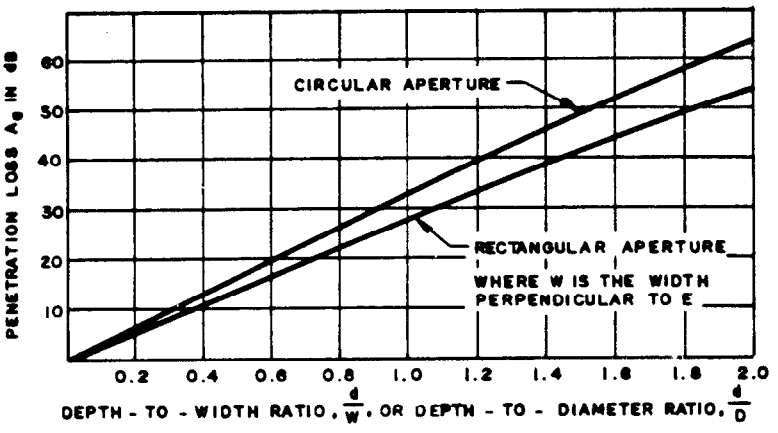

(a)

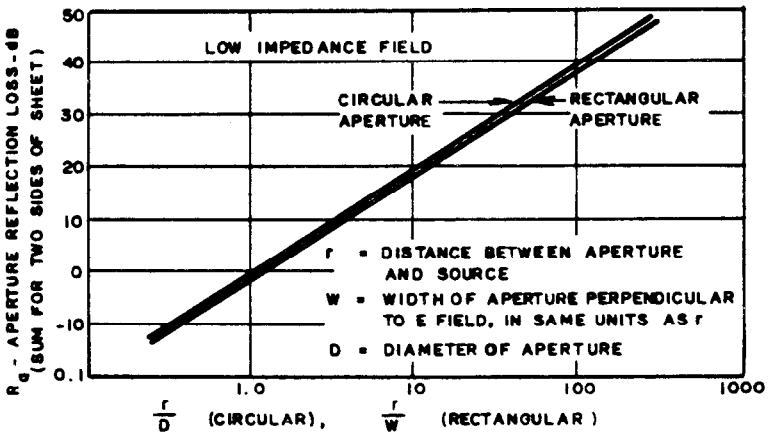

(b)

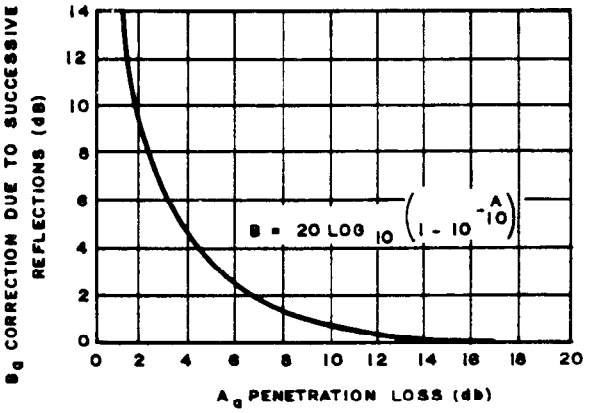

(c)

Figure 5-18. Aperture shielding. (sheet 1 of 2)

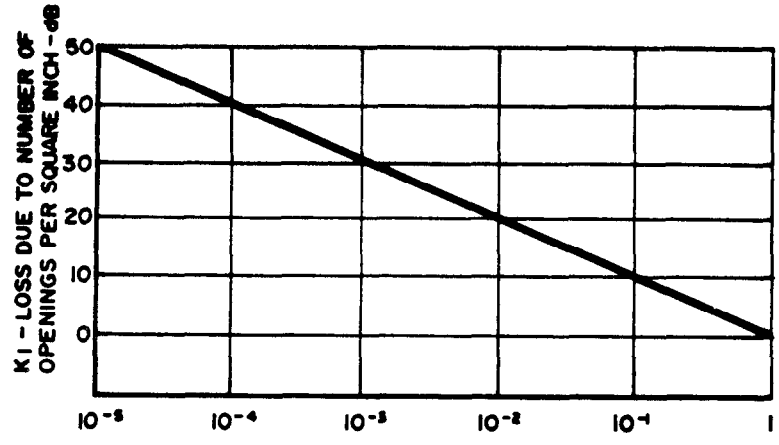

$K_1 = -10 \log an$, $r \gg W, D$

a = AREA OF SINGLE APERTURE

n = NUMBER OF APERTURES PER SQUARE INCH

r = DISTANCE BETWEEN SOURCE AND APERTURES

W = WIDTH OF RECTANGULAR APERTURES, PERPENDICULAR TO FIELD

D = DIAMETER OF CIRCULAR APERTURES

(d)

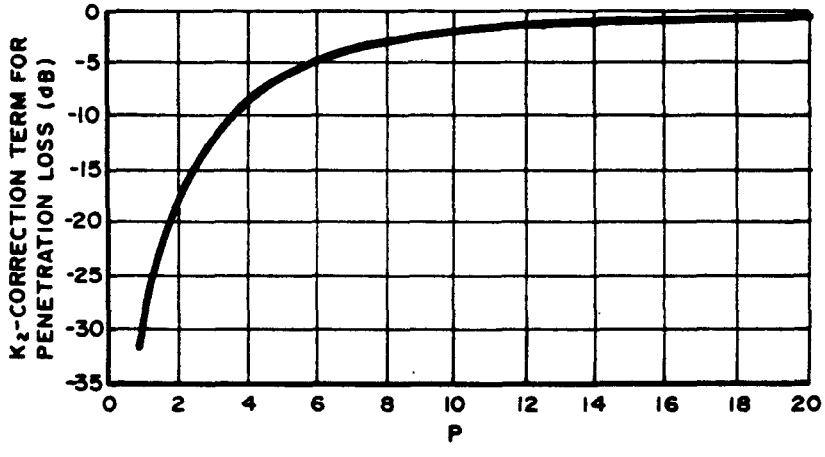

$P = \frac{\text{WIRE DIAMETER}}{\text{SKIN DEPTH}}$ FOR SCREENING

$= \frac{\text{CONDUCTOR WIDTH BETWEEN HOLES}}{\text{SKIN DEPTH}}$

FOR PERFORATED SHEETS

$K_2 = -20 \log_{10} (1 + 35P^{-2.3})$

(e)

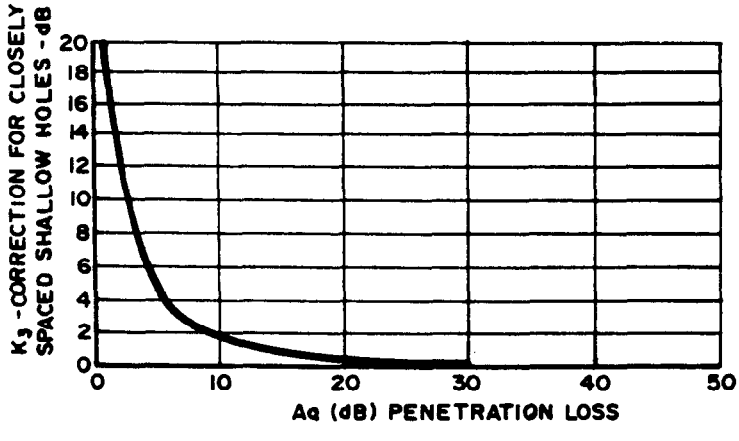

$K = 20 \log \left(\coth \frac{A\alpha}{8.686} \right)$

(f)

Figure 5-18. Aperture shielding. (sheet 2 of 2)

This page not used.

This page not used.

This page not used.

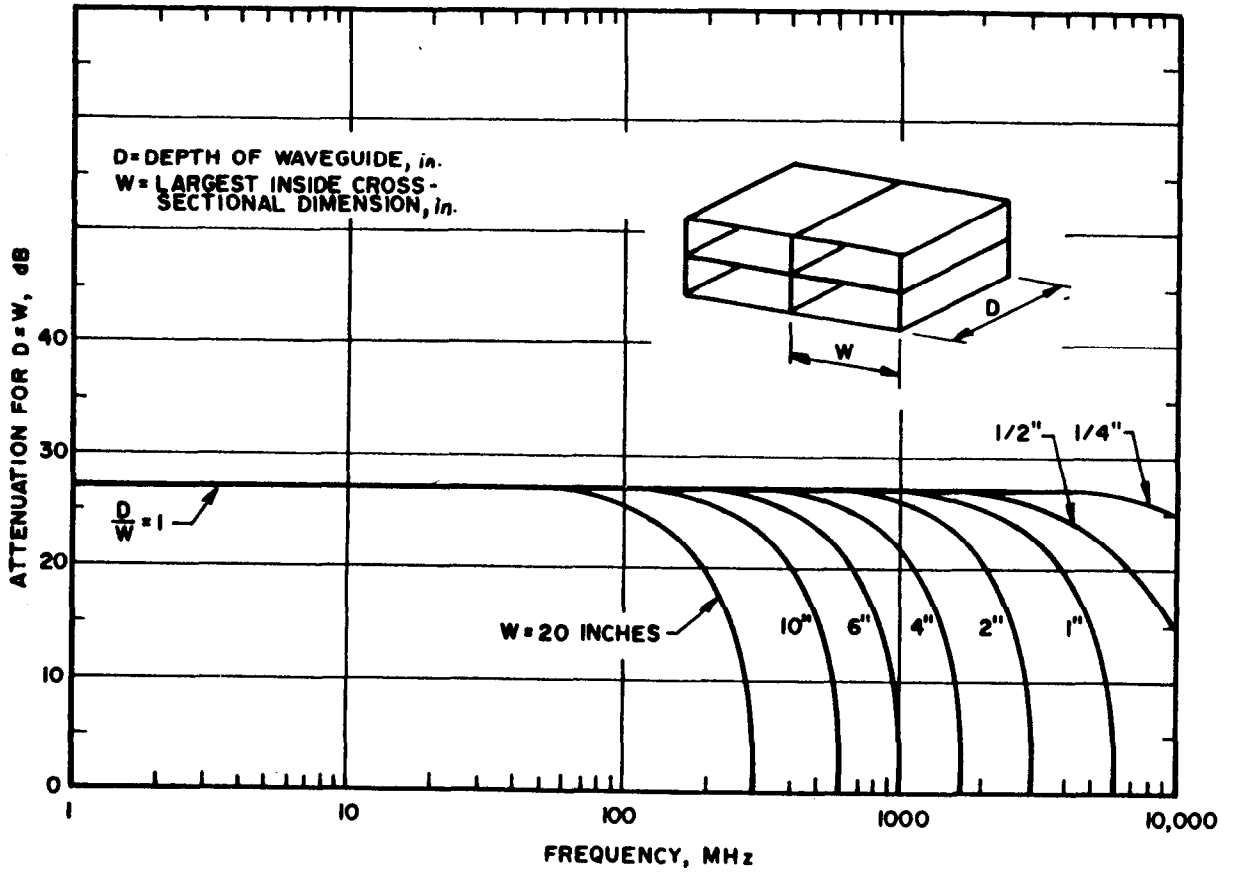

Figure 5-22. Attenuation--rectangular waveguide. (Source: ref 5-3)

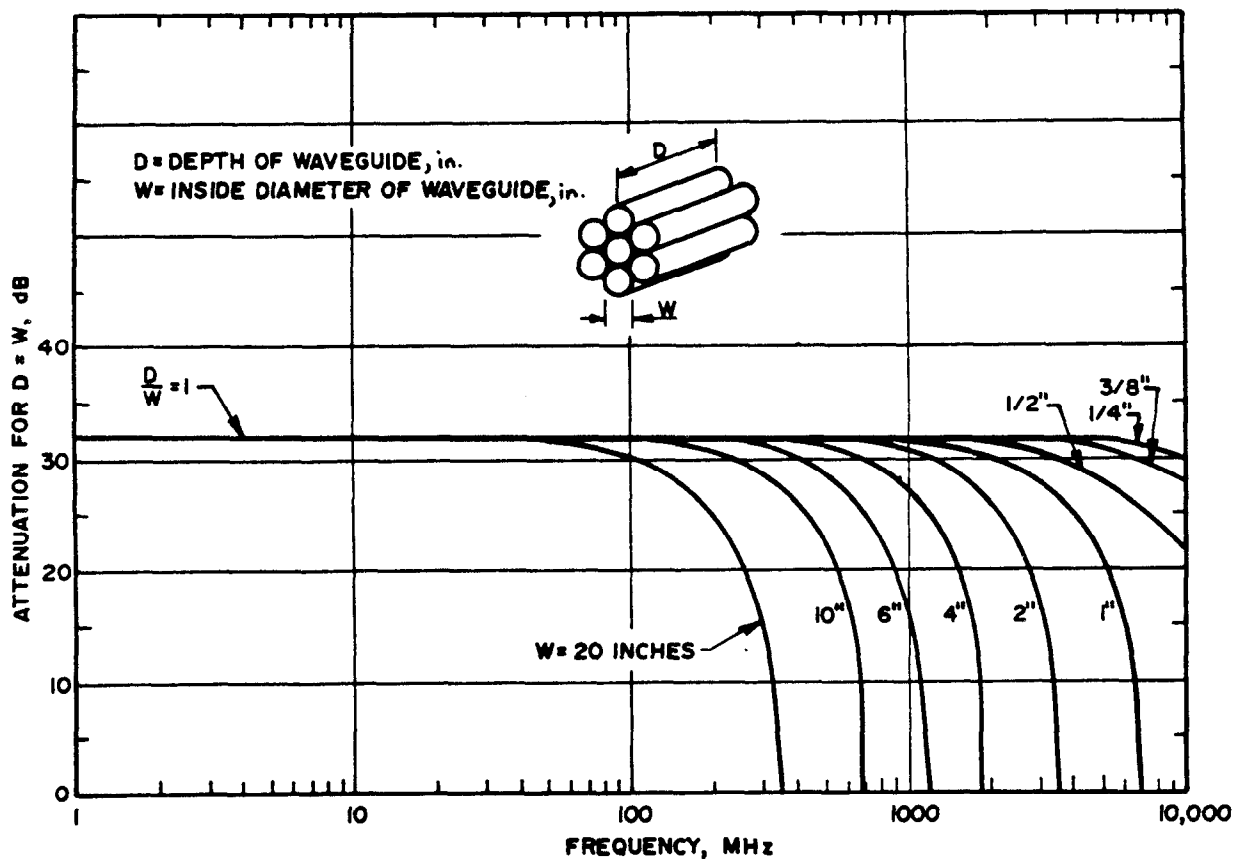

Figure 5-23. Attenuation--circular waveguide. (Source: ref 5-3)

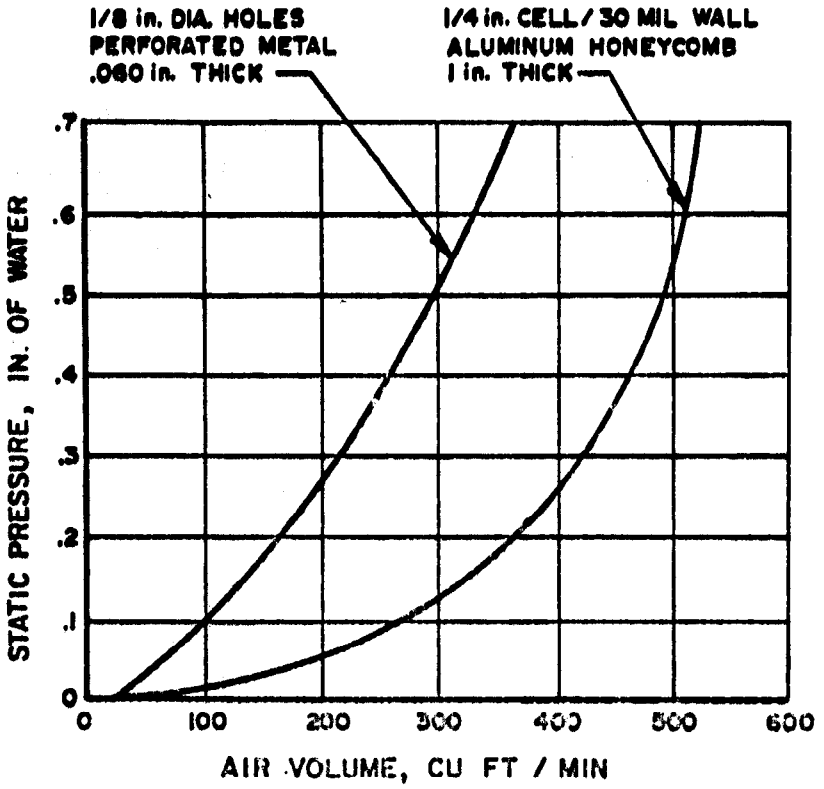

Figure 5-24. Air impedance of perforated metal and honeycomb. (Source: ref 5-3)

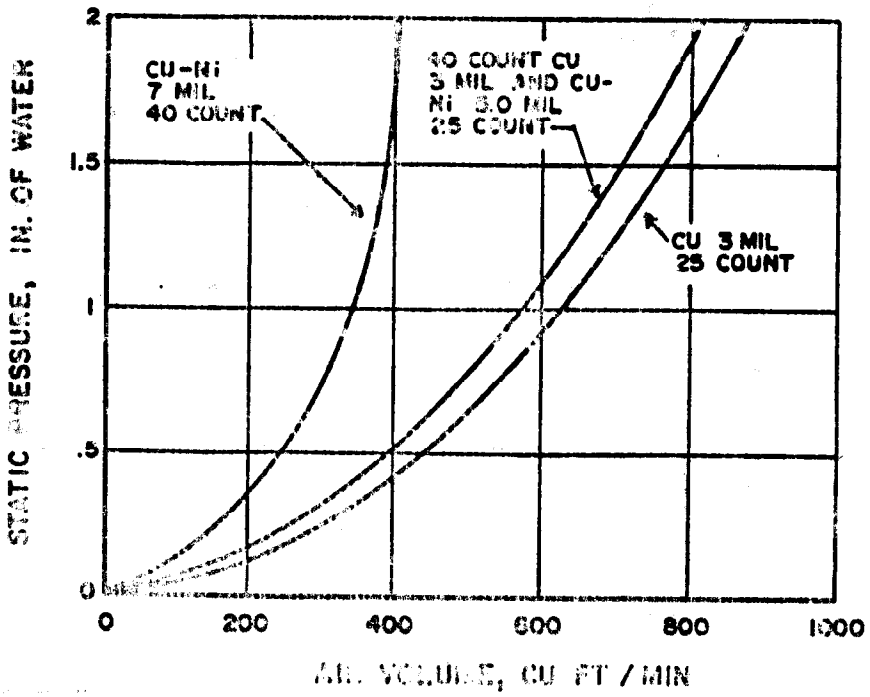

Figure 5-25. Air impedance of copper and nickel mesh. (Source: ref 5-3)

This page not used.

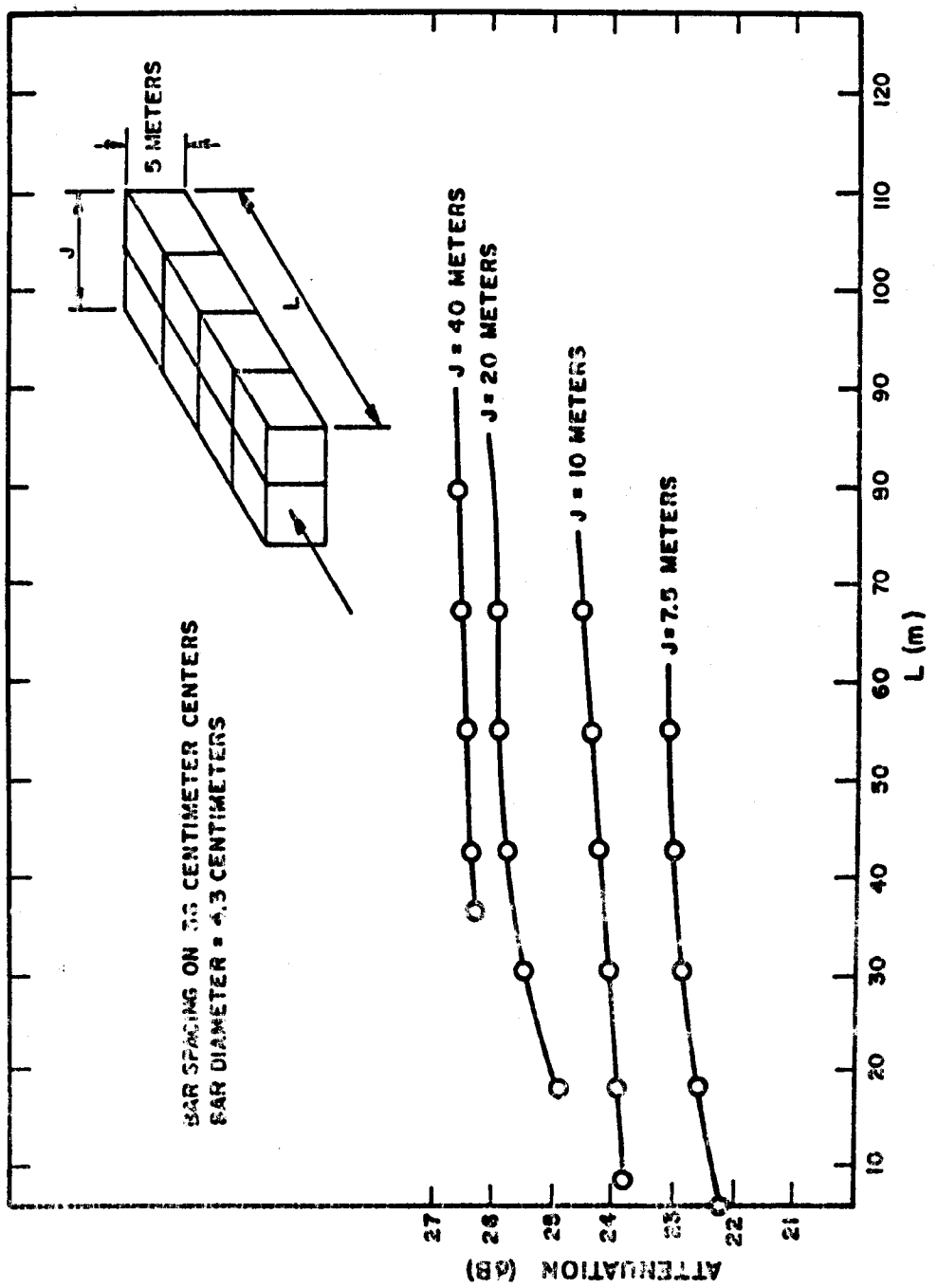

Figure 5-27. Center area attenuation of 5-meter-high, single-course reinforcing steel room. (Source: ref 5-7)

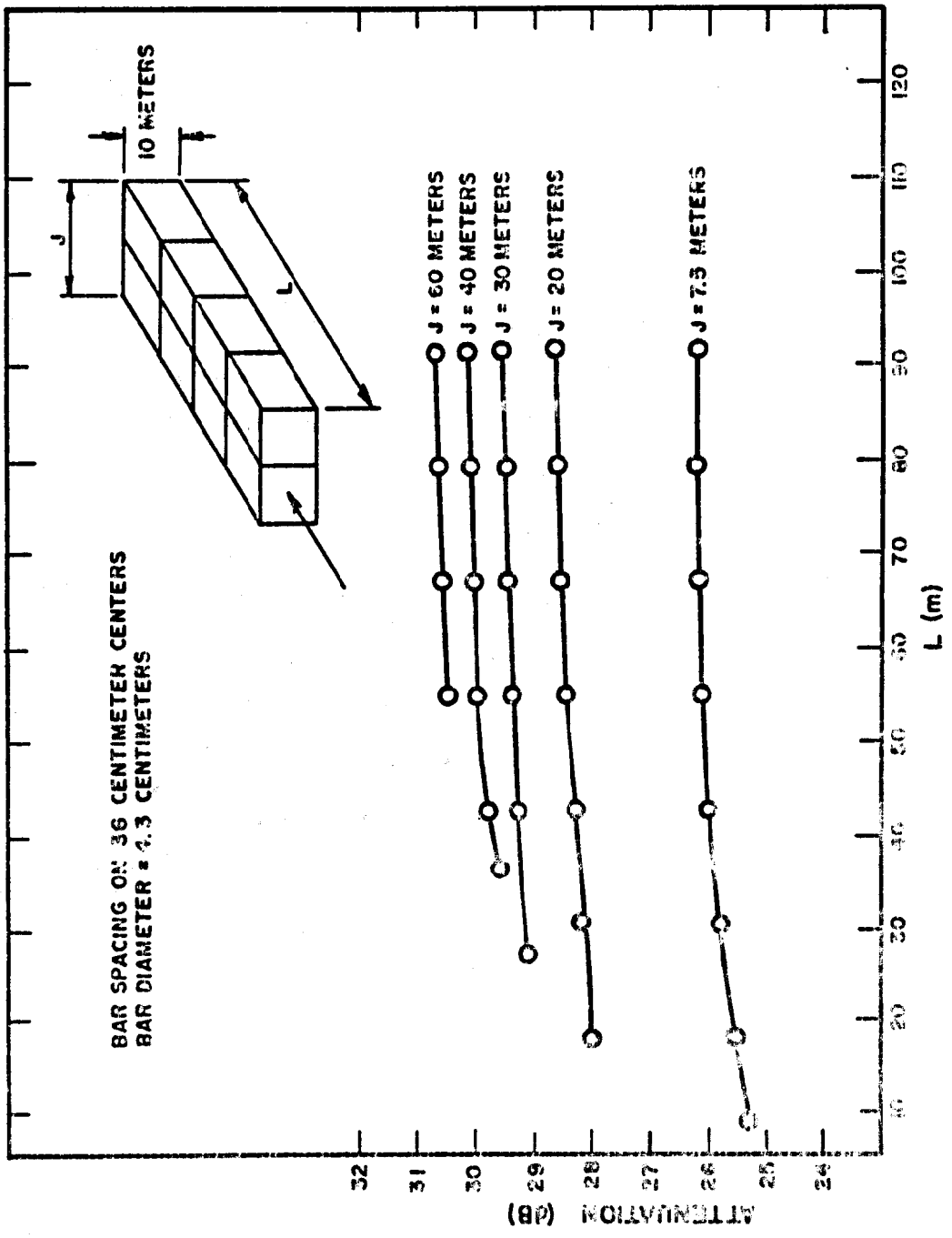

Figure 5-28. Center area attenuation of 10-meter-high, single-course reinforcing steel room. (Source: ref 5-7)

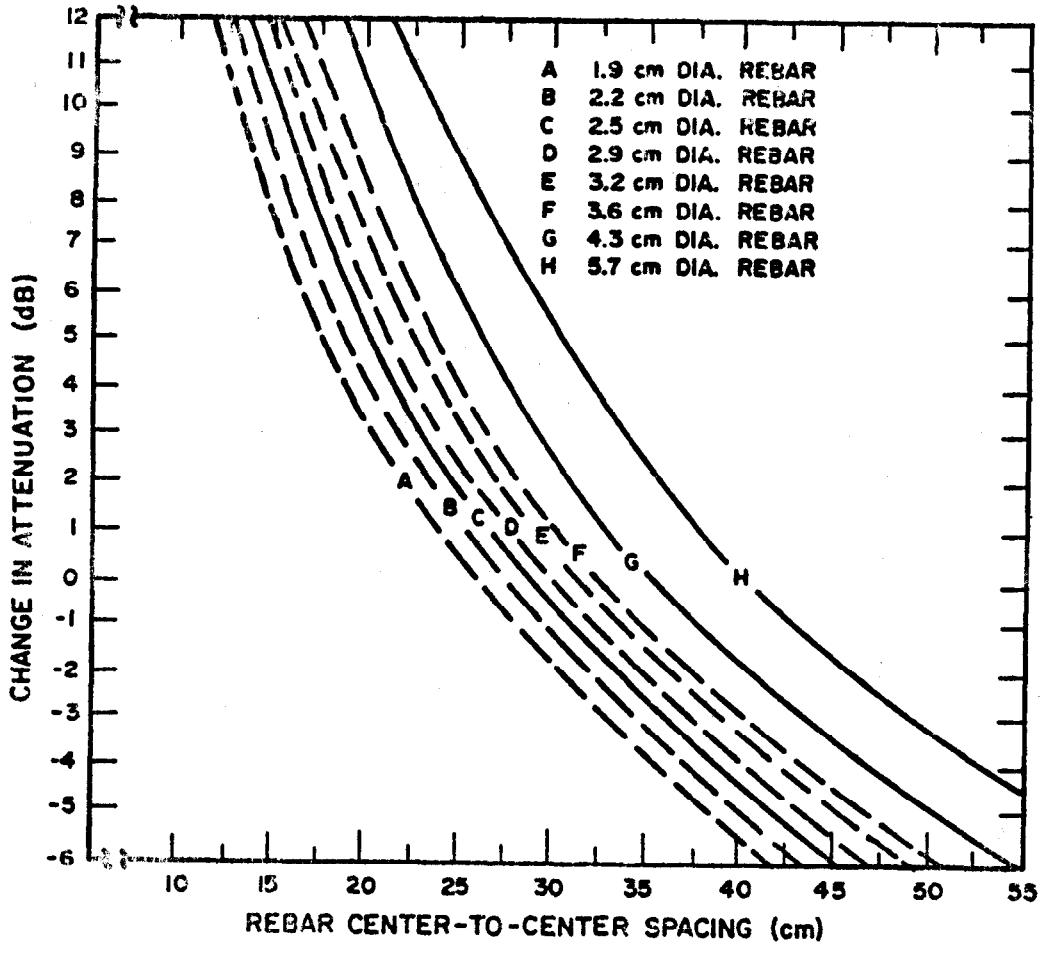

Figure 5-29. Correction curves for various rebar diameters and spacings using single-course rebar construction. (Source: ref 5-7)

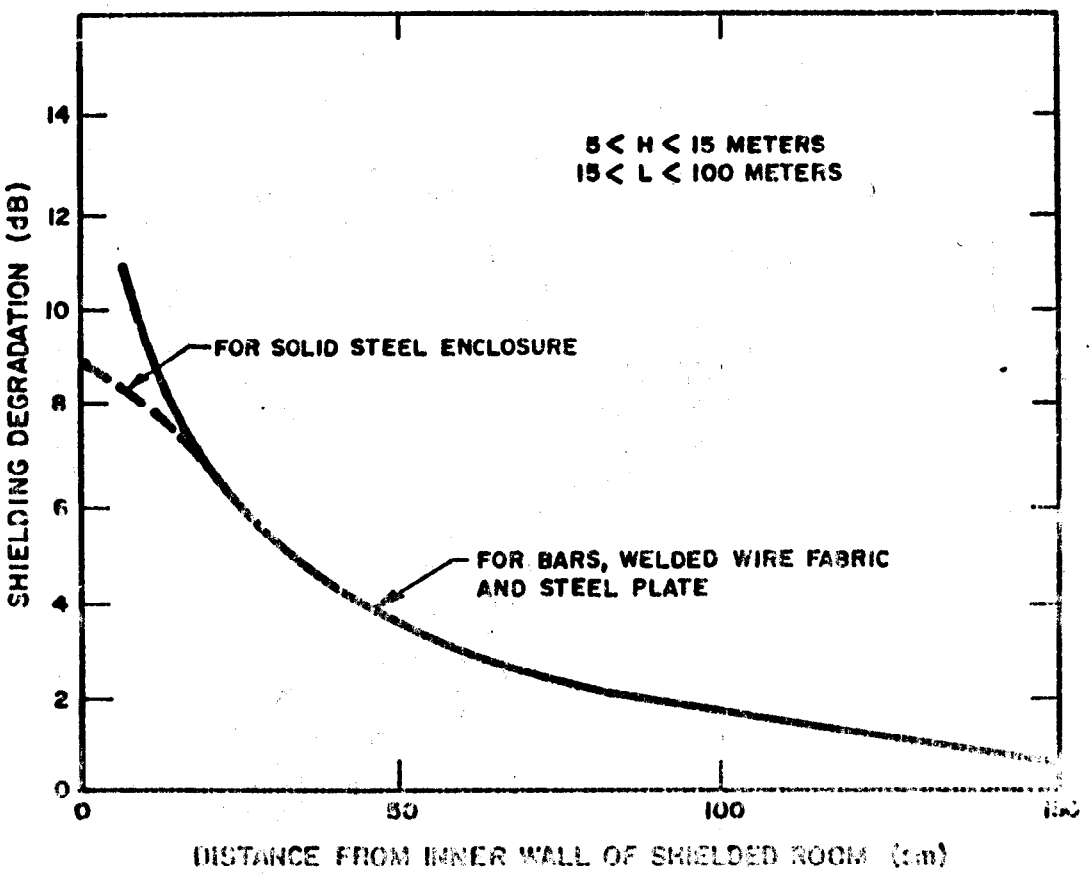

Figure 5-30. Shielding degradation versus distance from wall. (Source: ref 5-7)

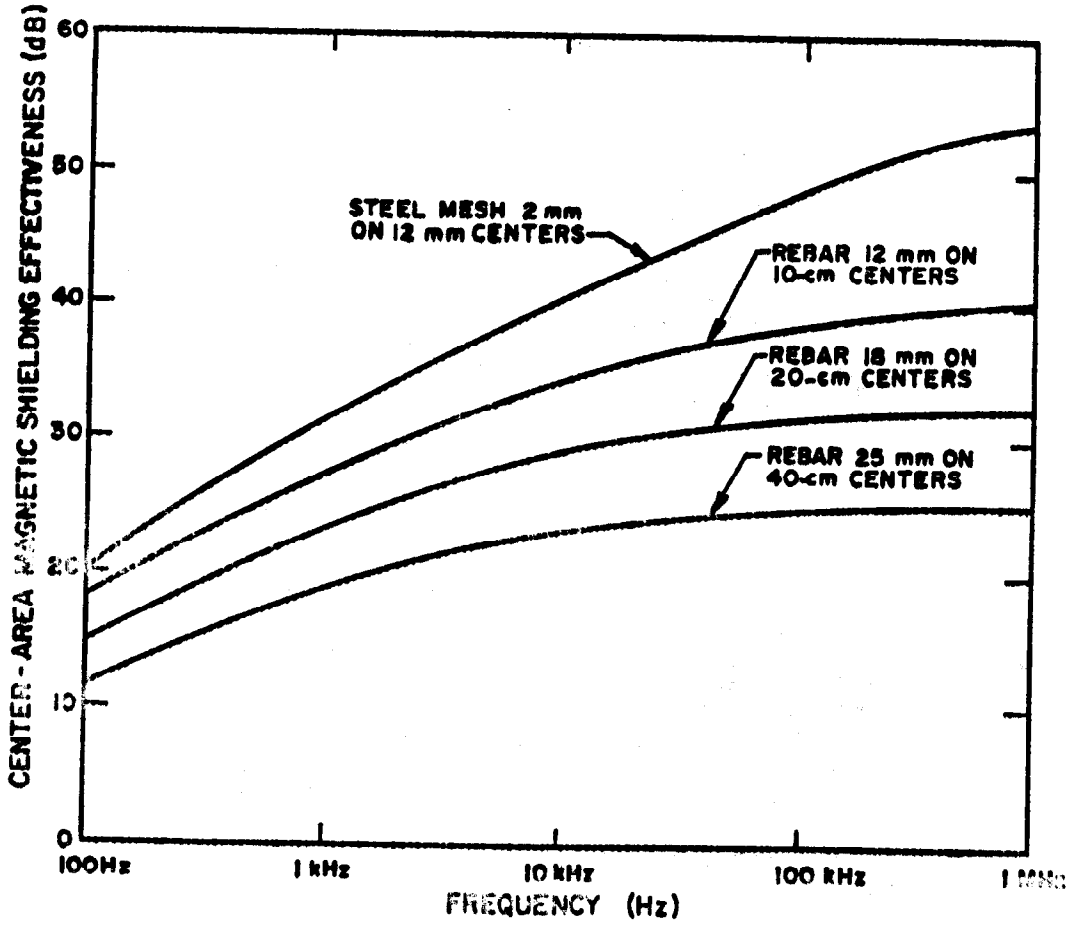

Figure 5-31. Shielding effectiveness of reinforcement steel. (Source: ref 5-7)

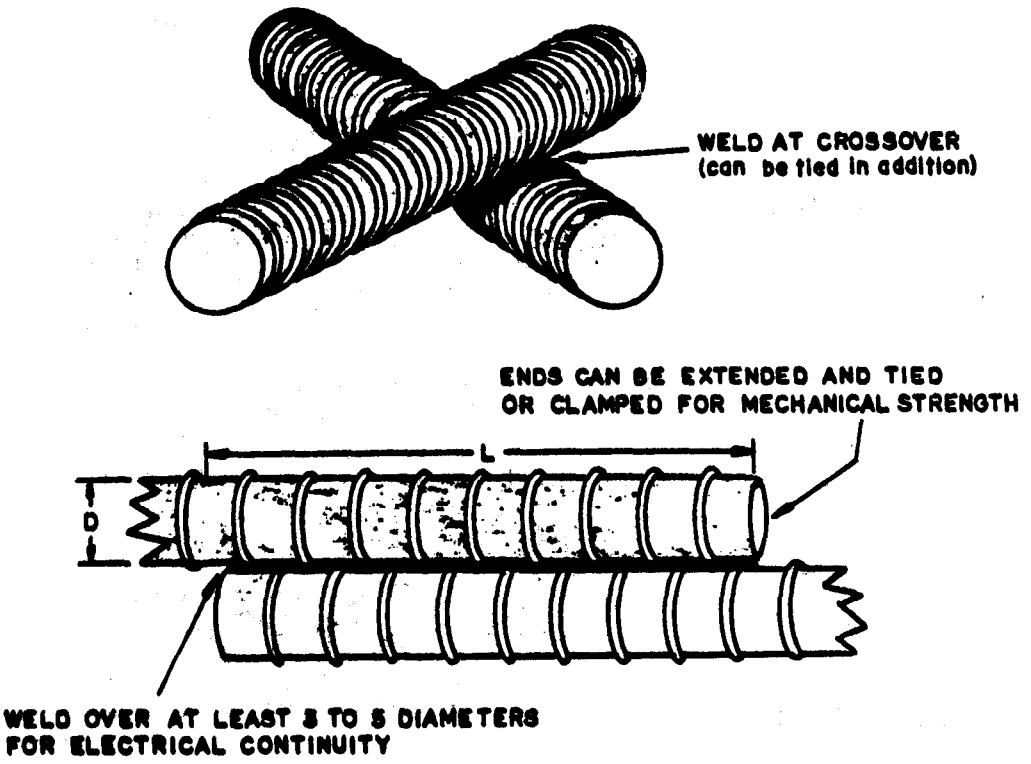

Figure 5-32. Reinforcement steel welding practice. (Source: ref 5-7)

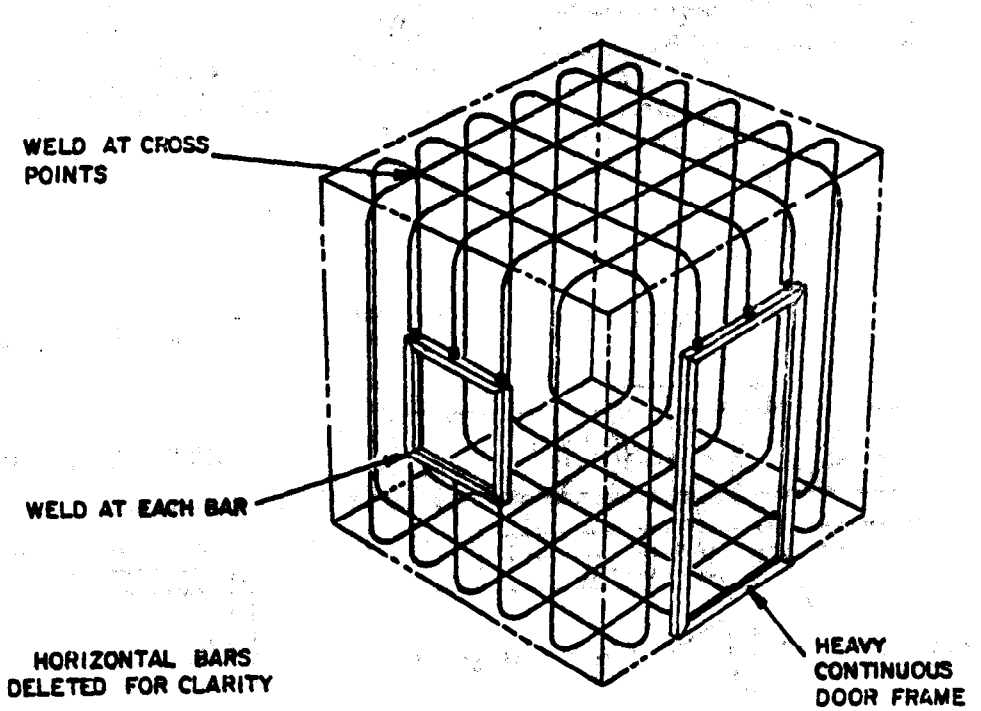

Figure 5-33. Schematic presentation--reinforcement steel shield. (Source: ref 5-7)

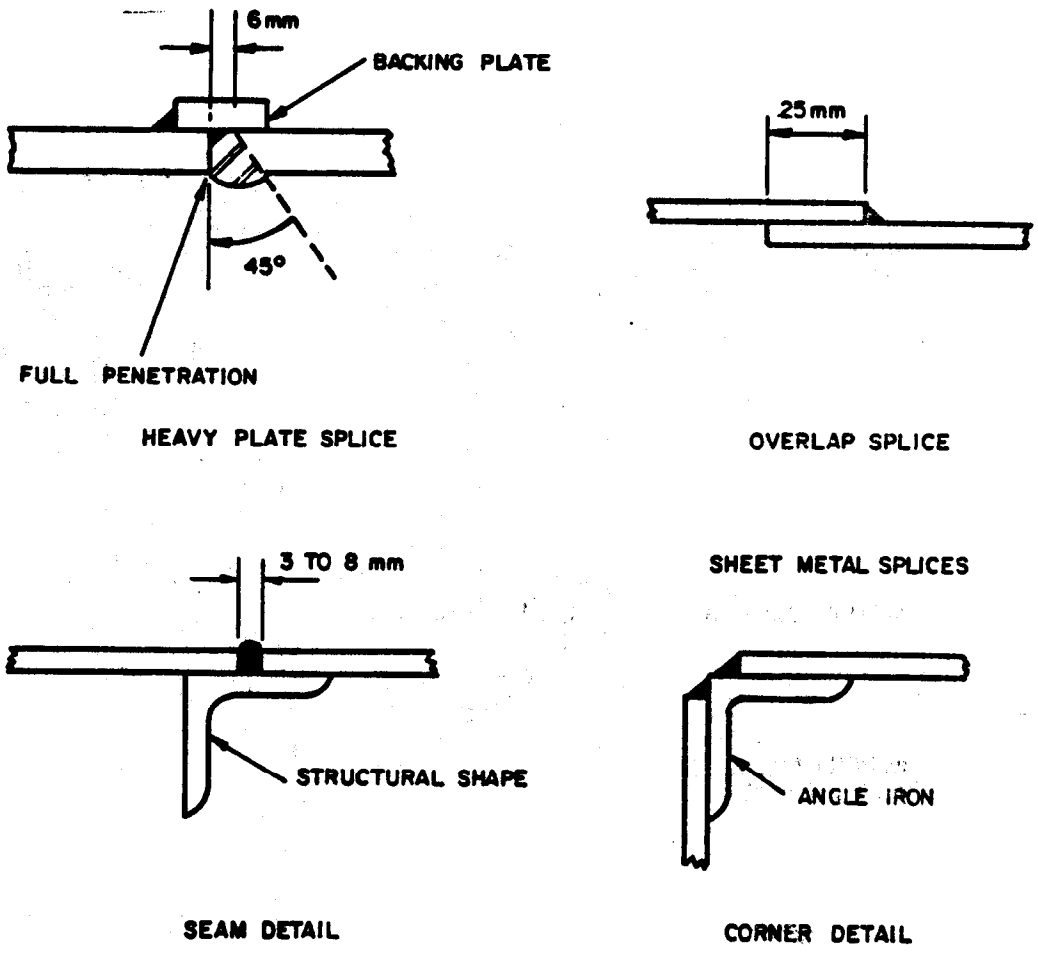

Figure 5-34. Weld joints for sheet steel shields. (Source: ref 5-7)

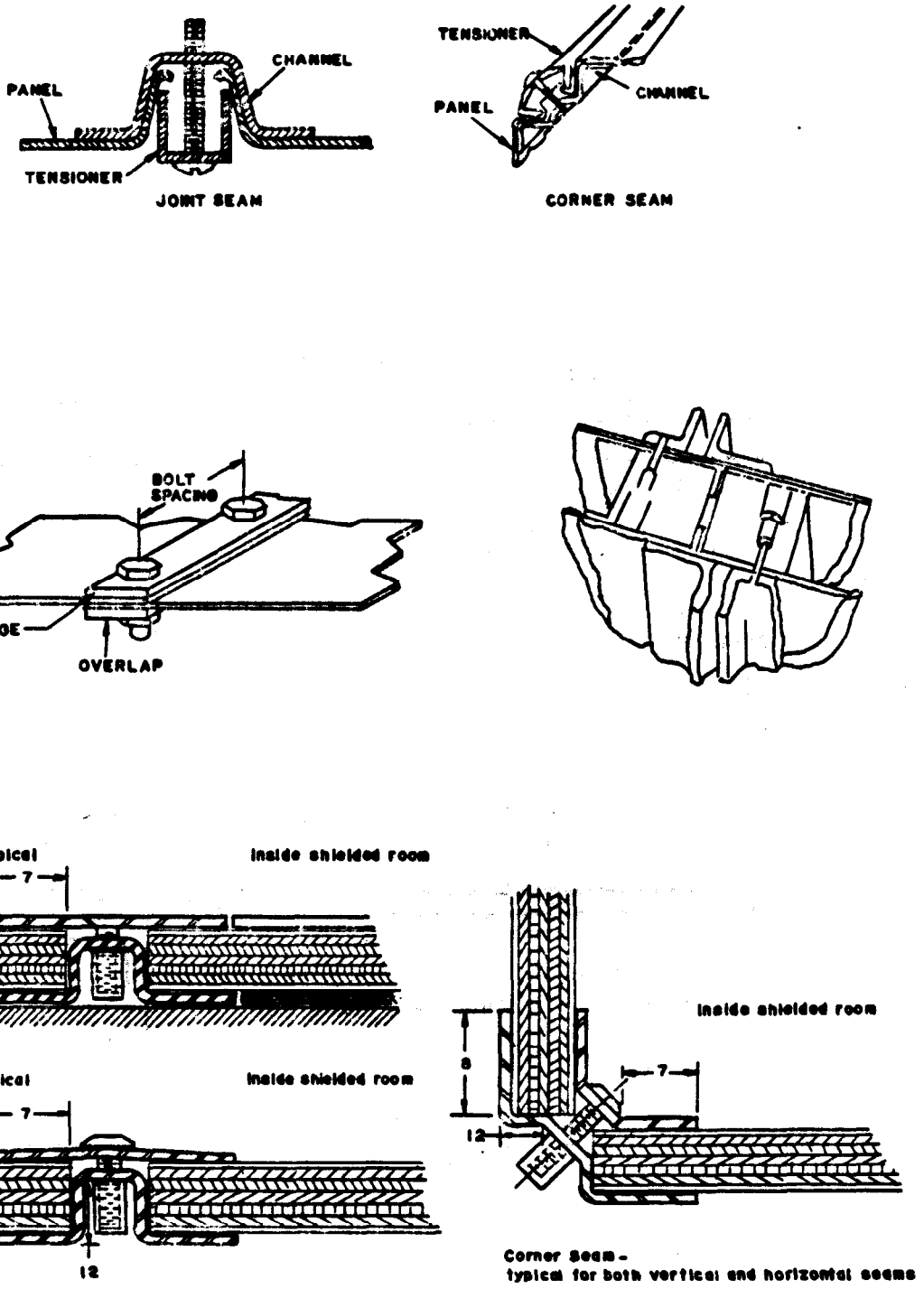

Figure 5-35. Bolted joints for metallic shields. (Source: ref 5-7)

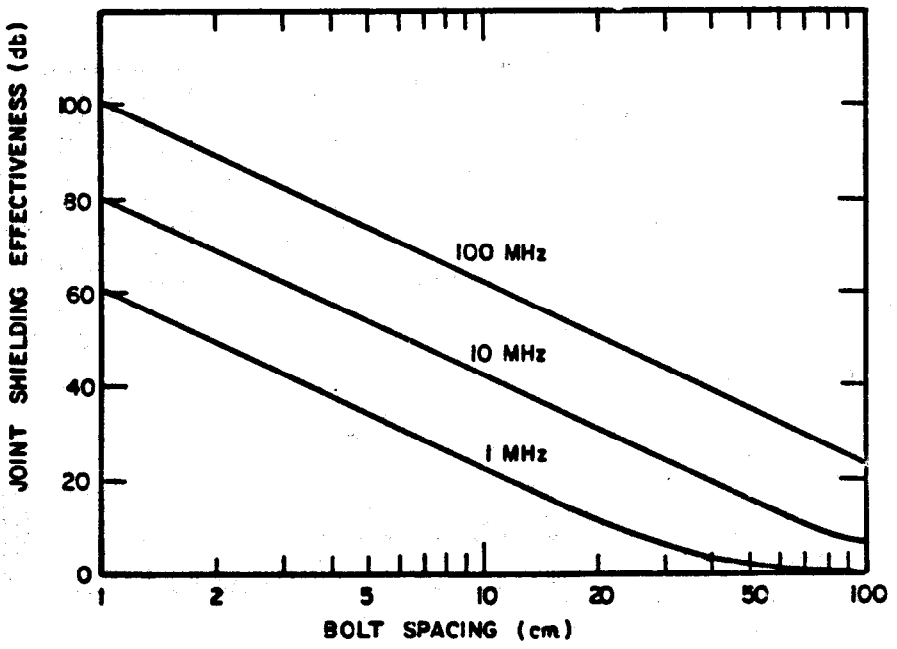

Figure 5-36. Shielding effectiveness for bolted joints. (Source: ref 5-7)

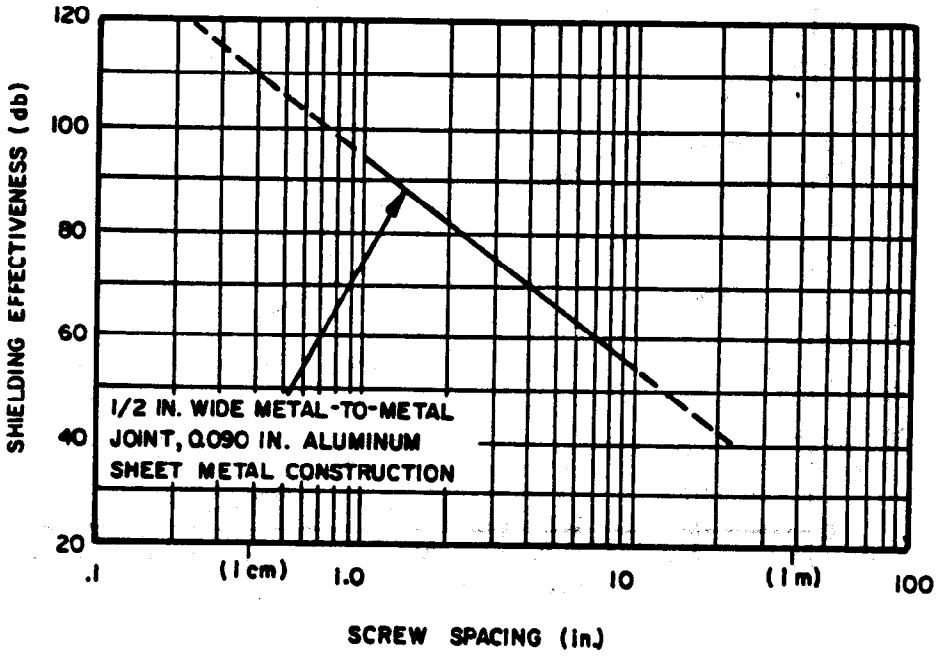

Figure 5-37. Influence of screw spacing on shielding effectiveness. (Source: ref 5-6)

Deflection	W Diam
.007 - .018	.070
.010 - .026	.103
.013 - .031	.125
.014 - .035	.139

Deflection	H
.006 - .012	.068
.008 - .016	.089
.012 - .024	.131
.014 - .029	.156
.016 - .032	.175

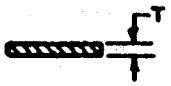

Deflection	T
.001 - .002	.020
.001 - .003	.032
.003 - .006	.062
.003 - .009	.093

Deflection	A
.025 - .080	.200
.030 - .125	.250
.075 - .250	.360

Figure 5-38. Gasket deflection limits (in inches). (Source: ref 5-30)

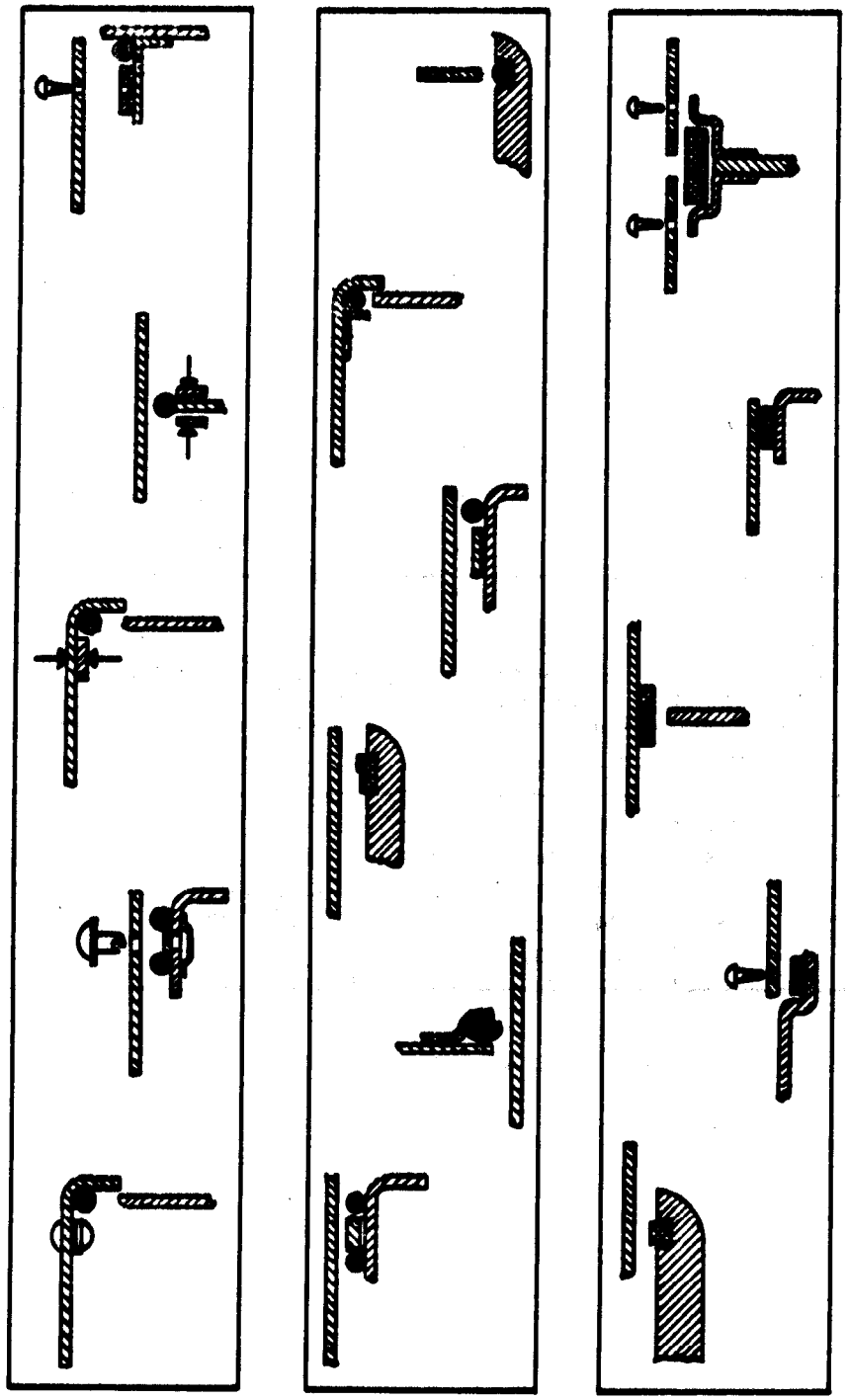

Figure 5-39. Typical mounting techniques for RF gaskets. (Source: ref 5-6)

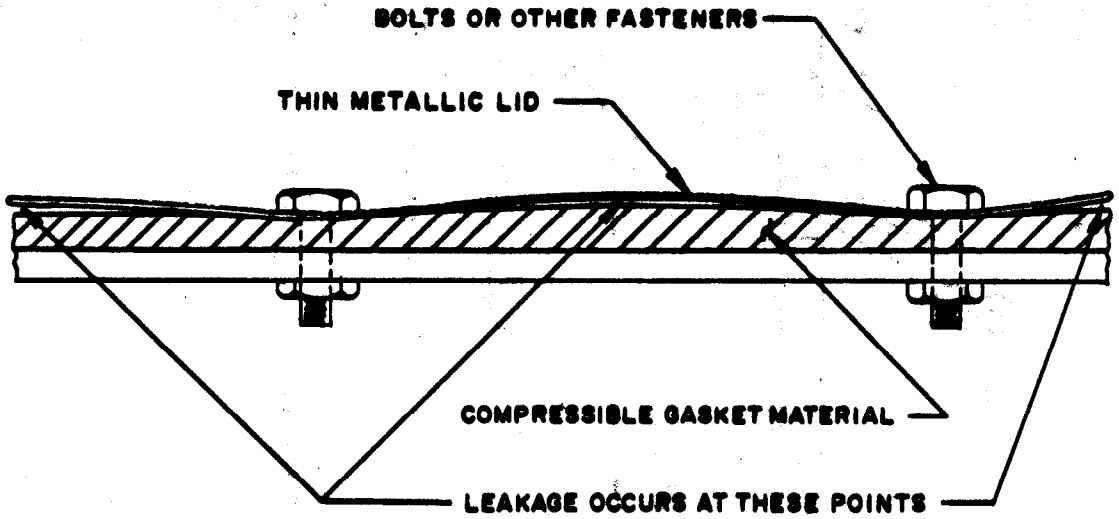

NOTE: VIEW PURPOSELY EXAGGERATED TO DEMONSTRATE IMPERFECT SEAL CONDITIONS.

Figure 5-40. Improper gasket application. (Source: ref 5-3)

NOT TO SCALE

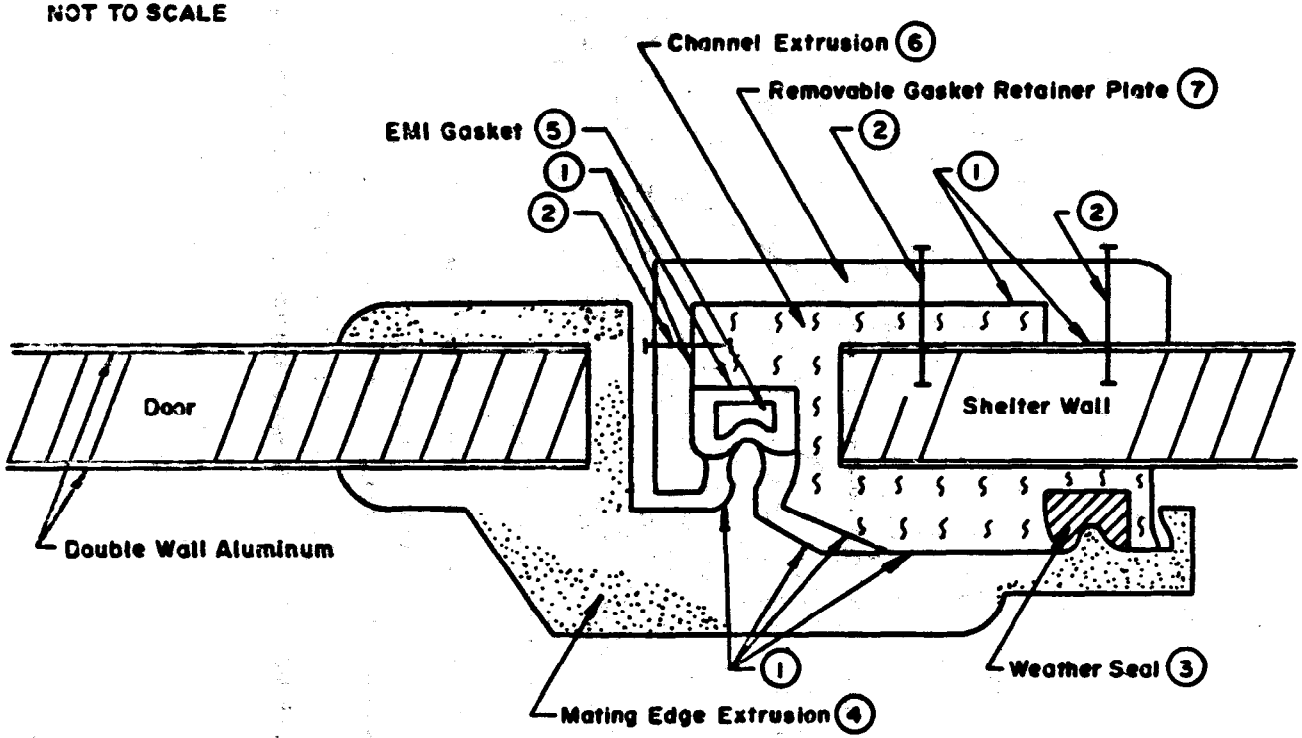

① = Surfaces with Tin Coating or Plating

② = Bolts or Screws to Affix Retainer Plate

③ = Silicone, Hollow Extrusion Elastomer

④ = Aluminum Extrusion Welded to Door

⑤ = Knitted Wire Mesh Gasket with Hollow "D" Elastomer

⑥ = Aluminum Extrusion Welded to Shelter Wall

⑦ = Aluminum Extrusion Plate Bolted to Channel Extrusion

Figure 5-41. EMI shielded door seam (mesh gasket). (Source: ref 5-8)

NOT TO SCALE

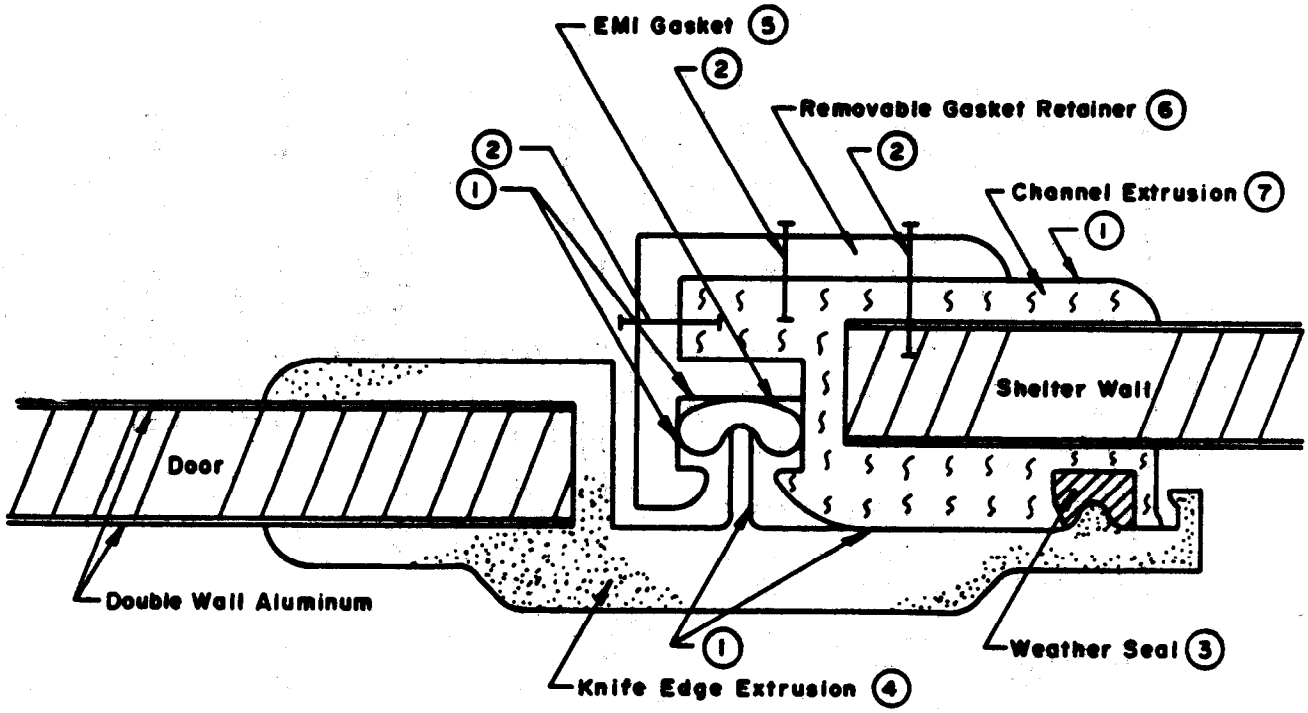

① = Surfaces with Tin Coating or Plating

② = Bolts or Screws to Affix Retainer Plate

③ = Silicone, Hollow Extruded Elastomer

④ = Aluminum Extrusion Welded to Door

⑤ = Tin-Plated Spiral "OVAL" Gasket

⑥ = Tin-Plated Aluminum Extrusion Gasket Retainer

⑦ = Aluminum Extrusion Welded to Shelter

Figure 5-42. EMI shielded door seam ("oval" spiral gasket). (Source: ref 5-8)

NOT TO SCALE

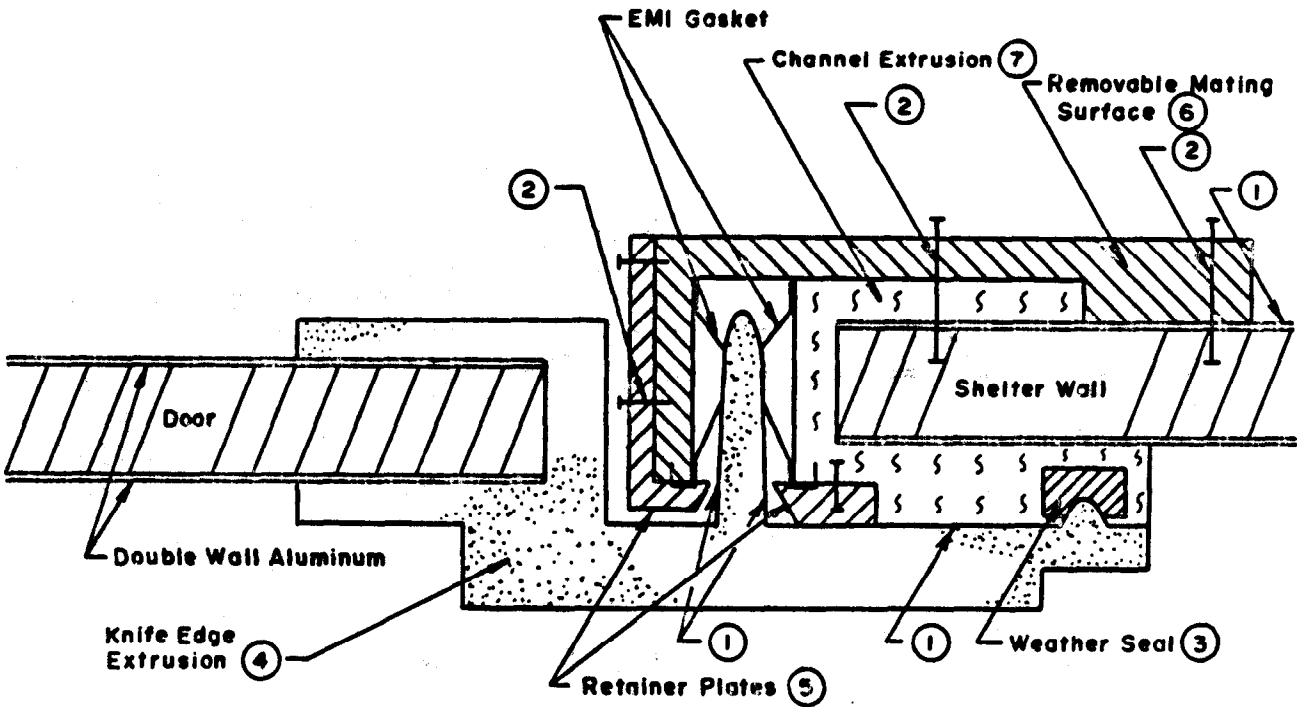

① = Surfaces with Tin Coating or Plating

② = Bolts or Screws to Affix Retainer Plates

③ = Silicone, Hollow Extrusion Elastomer

④ = Aluminum Extrusion Welded to Door

⑤ = Tin-Plated Aluminum Retainer Plates

⑥ = Aluminum Extrusion Bolted to Shelter (Removable)

⑦ = Aluminum Extrusion Welded to Shelter

Figure 5-43. EMI shielded door seam (fingerstock). (Source: ref 5-8)

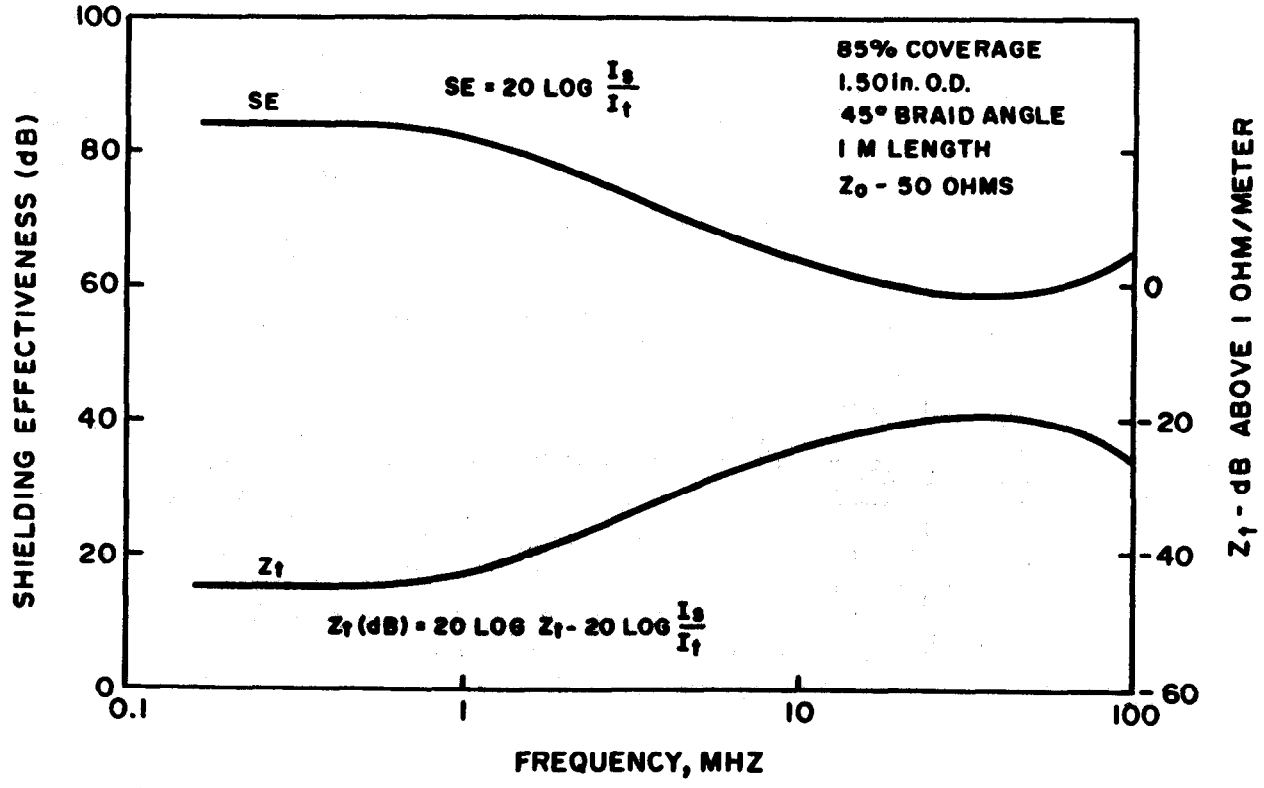

Figure 5-44. Shielding effectiveness and transfer impedance. (Source: ref 5-11)

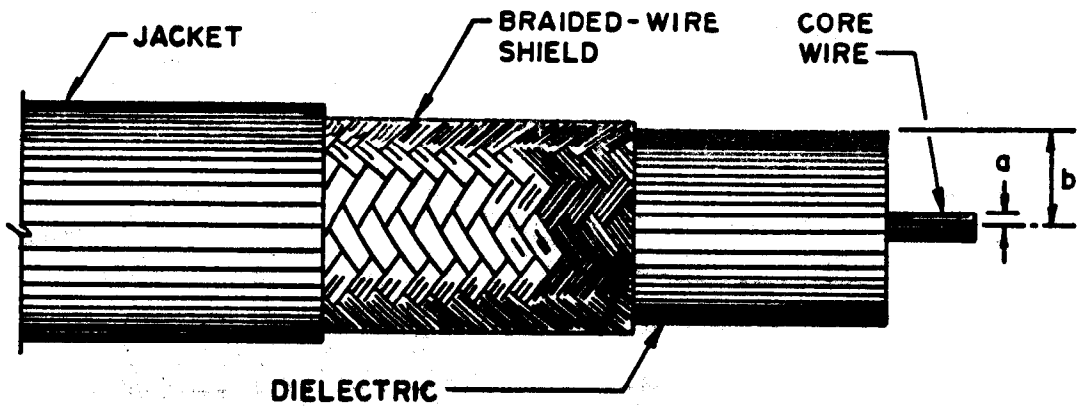

Figure 5-45. A braided-shield coaxial cable. (Source: ref 5-16)

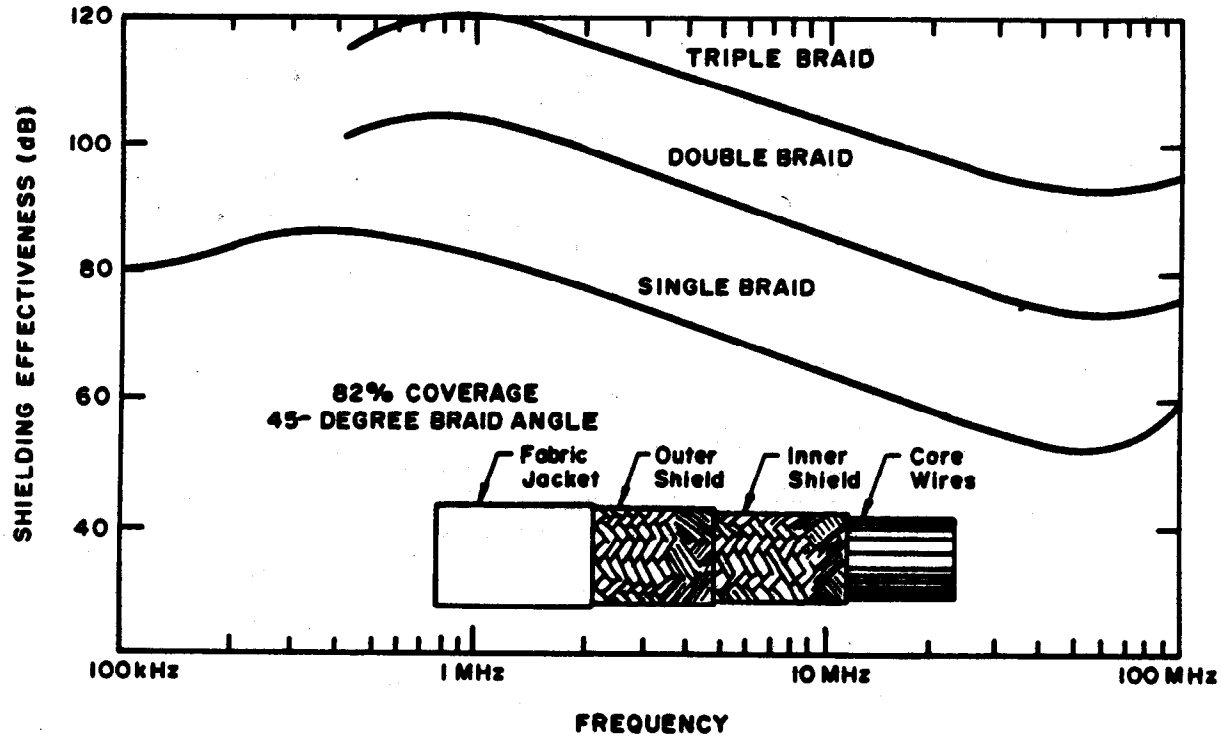

Figure 5-46. Cable shielding effectiveness with number of braid layers. (Source: ref 5-7)

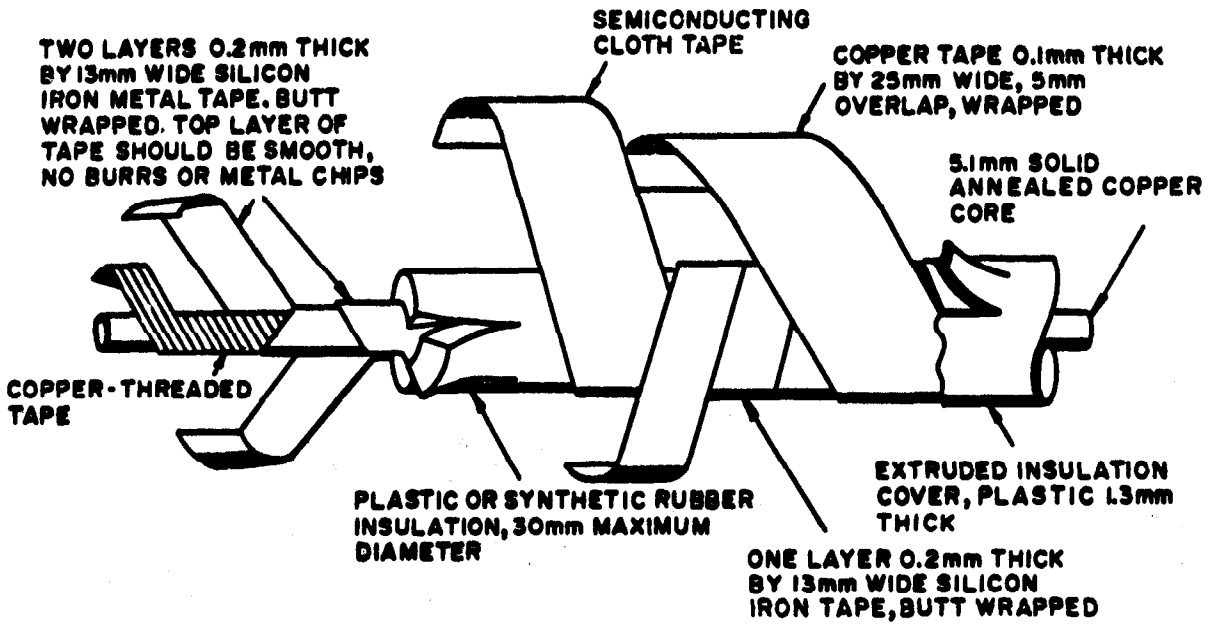

UNDERGROUND CABLE

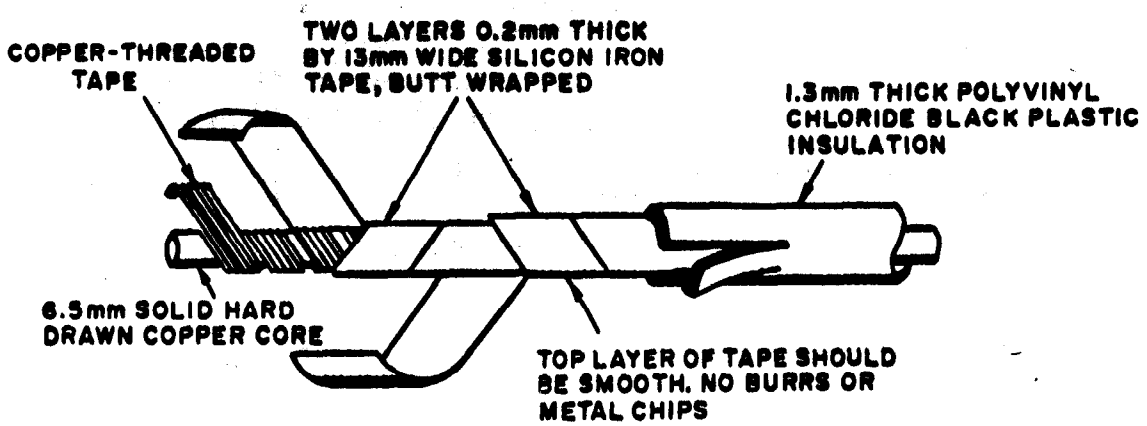

OVERHEAD CONDUCTOR

Figure 5-47. Lossy conductor construction. (Source: ref 5-7)

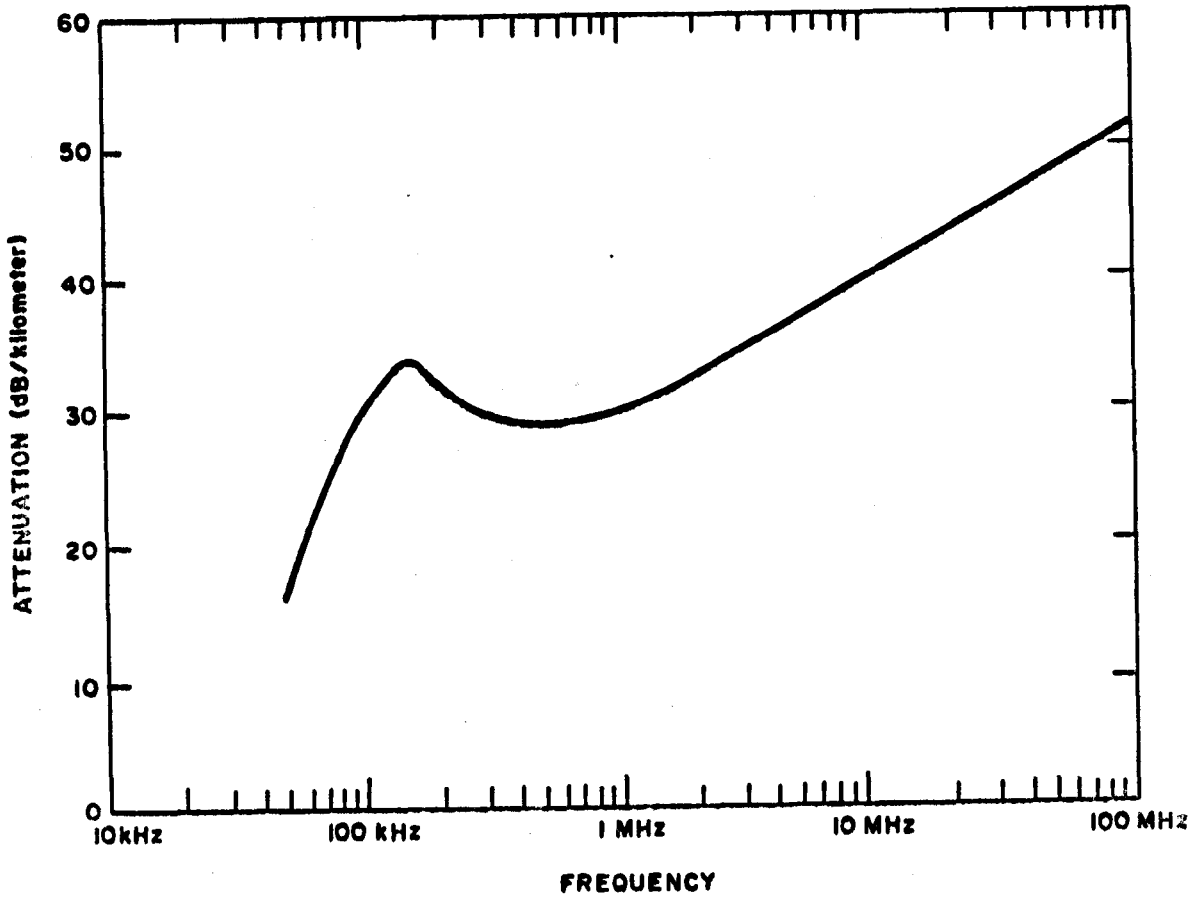

Figure 5-48. Attenuation of HEMP interference propagating on lossy-wrapped conductors. (Source: ref 5-7)

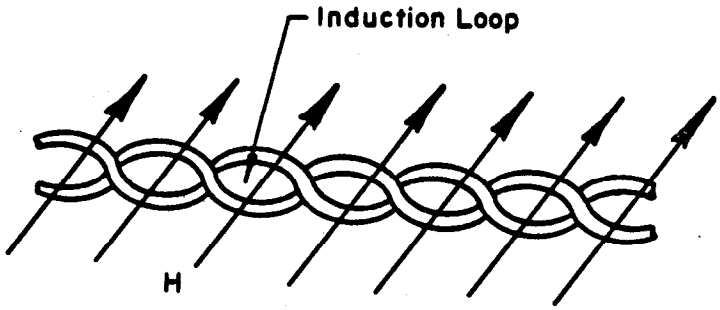

Figure 5-49. Induction loop area for twisted pair cables. (Source: ref 5-16)

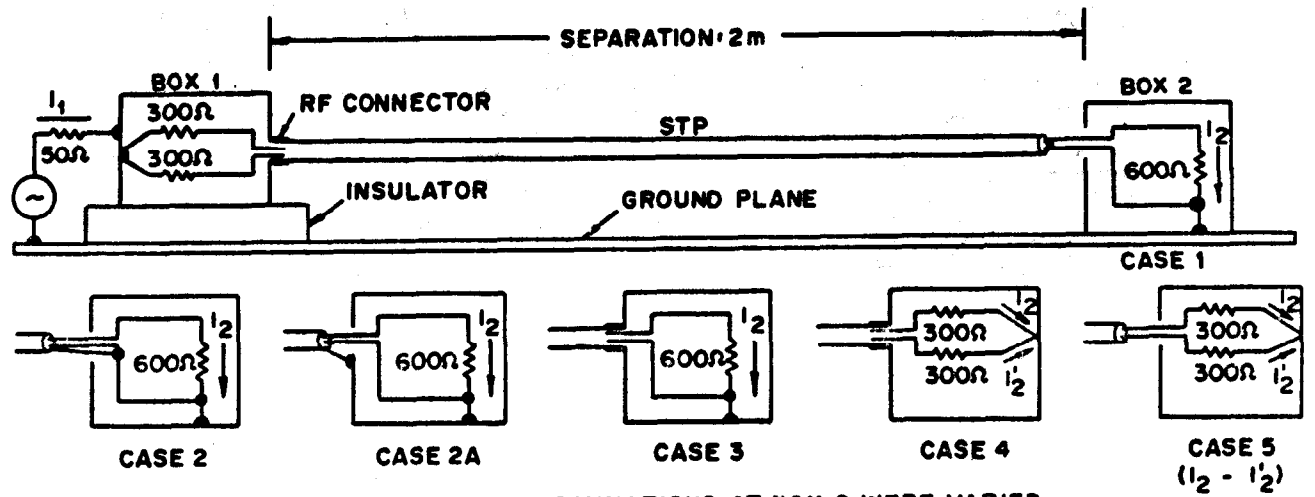

(a) TEST SETUP: ONLY TERMINATIONS AT BOX 2 WERE VARIED

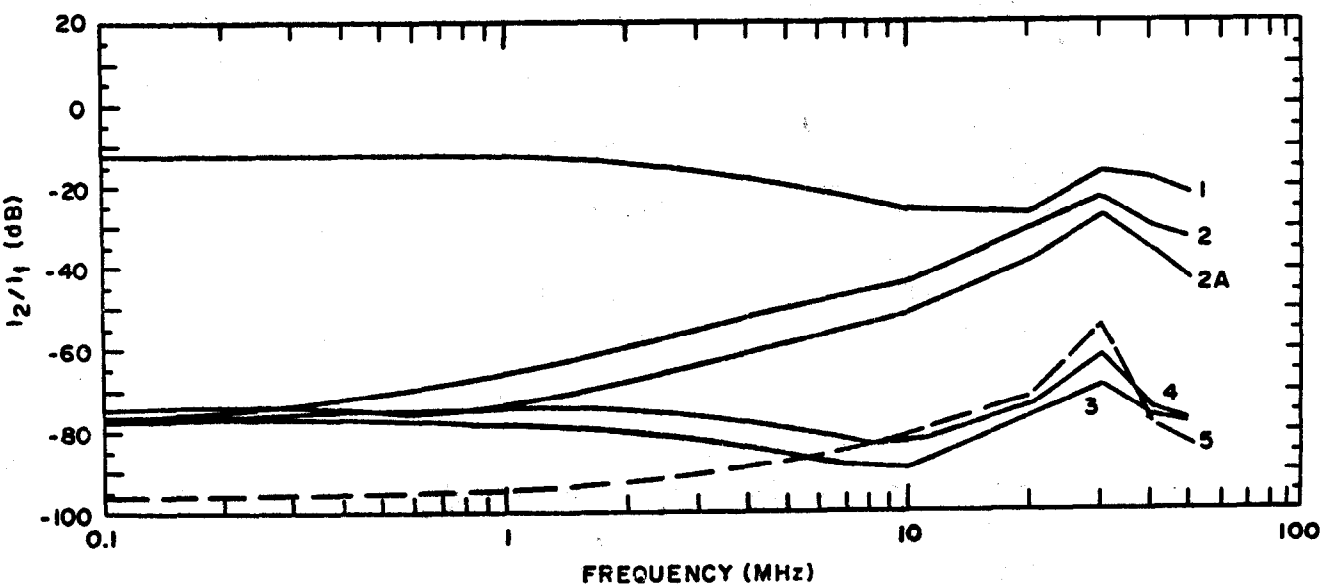

(1) NO SHIELD TERMINATION
(2) PIGTAIL, INSIDE
(2A) PIGTAIL, OUTSIDE
(3) RF CONNECTOR, UNBALANCED
(4) RF CONNECTOR, BALANCED
(5) NORMALIZED DIFFERENTIAL CURRENT
(no shield termination)

(b) NORMALIZED CURRENT I_2 (curve 5 shows the normalized differential current I_2 I'_2)

Figure 5-50. Experiments with shielded twisted pair cabling. (Source: ref 5-14)

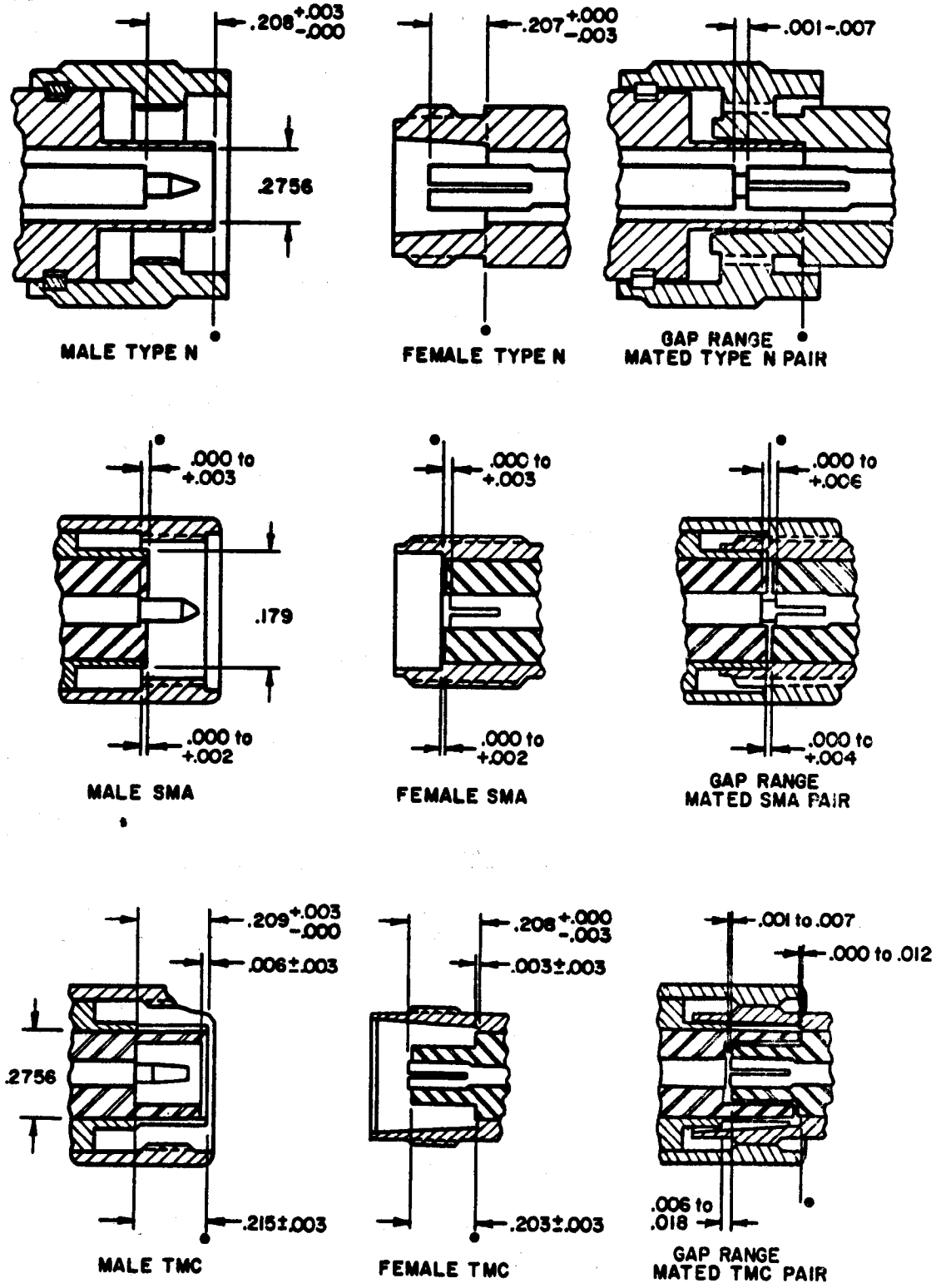

Figure 5-51. Construction of some popular coaxial connectors. (Source: ref 5-16)

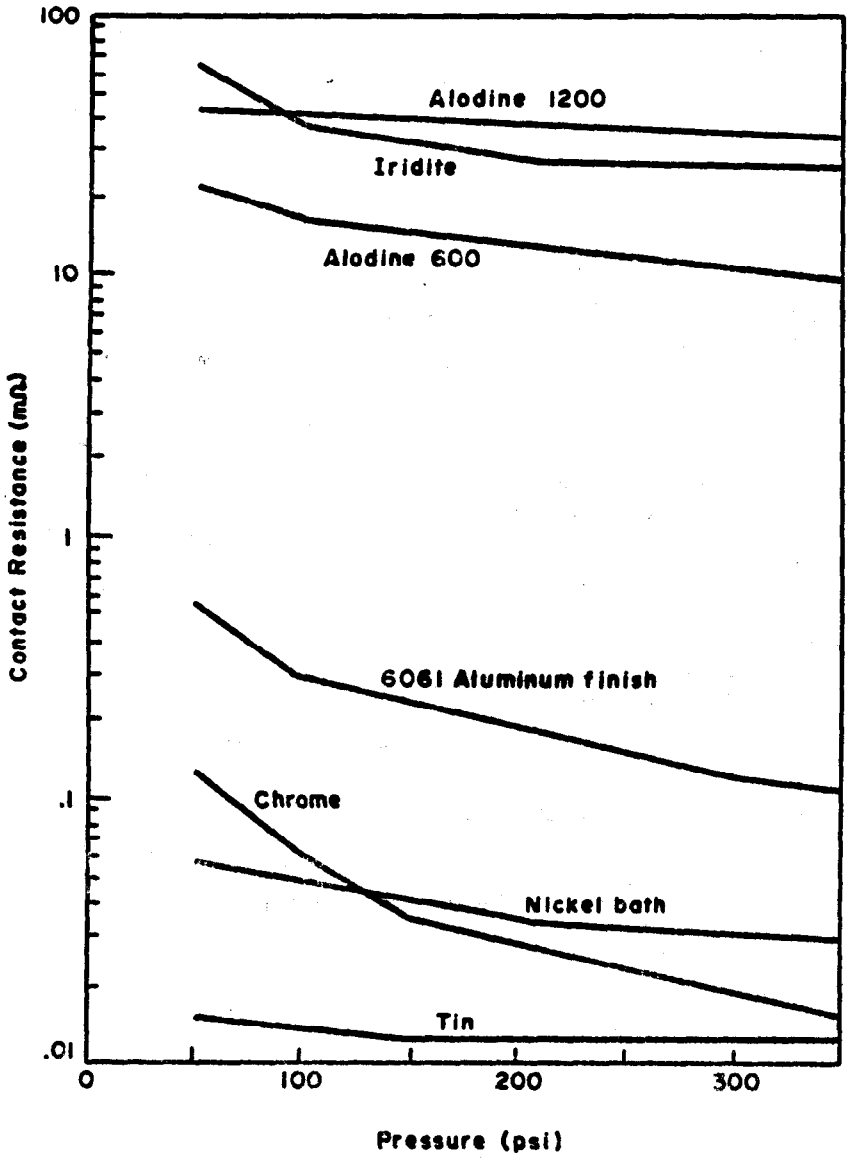

Figure 5-52. Contact resistance of conductive coatings on aluminum. (Source: ref 5-16)

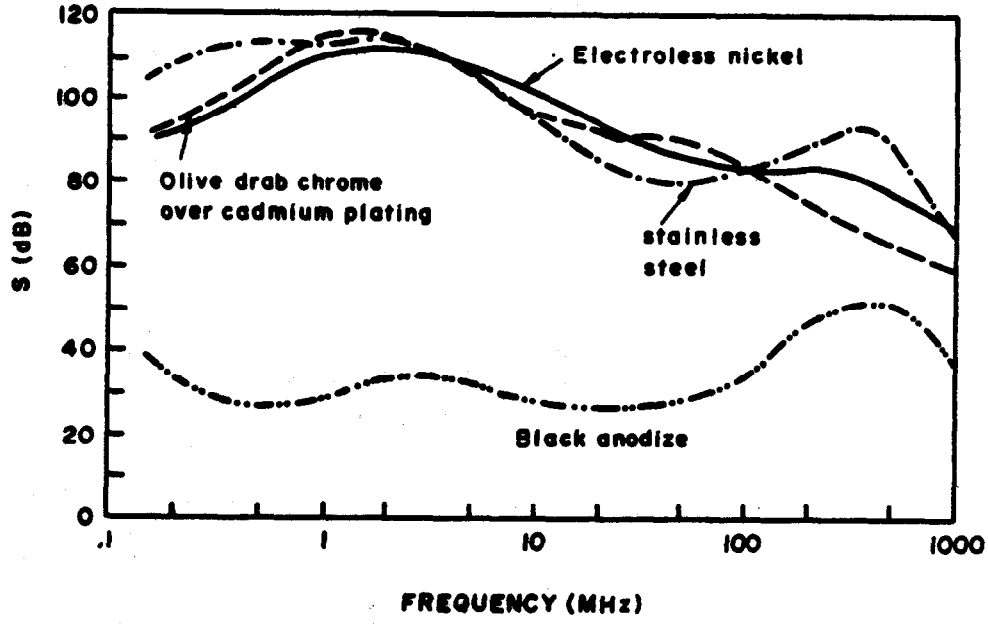

Figure 5-53. Shielding effectiveness of connectors with various finishes. (Source: ref 5-16)

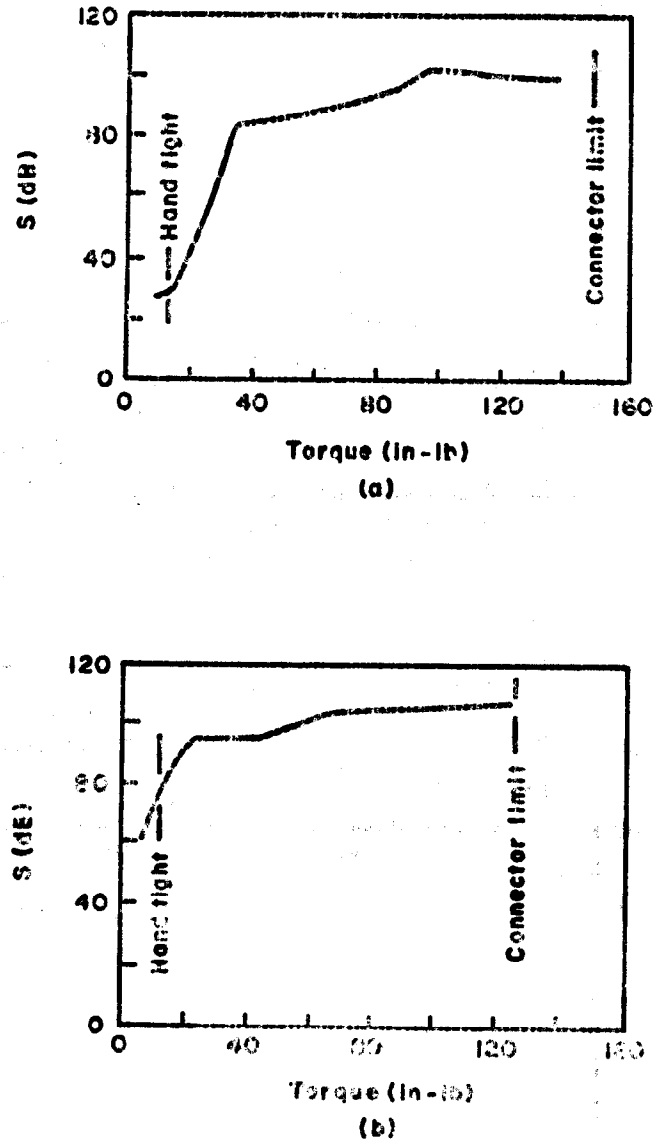

Figure 5-54. Effect of tightening torque on shielding effectiveness during vibration. (Source: ref 5-16)

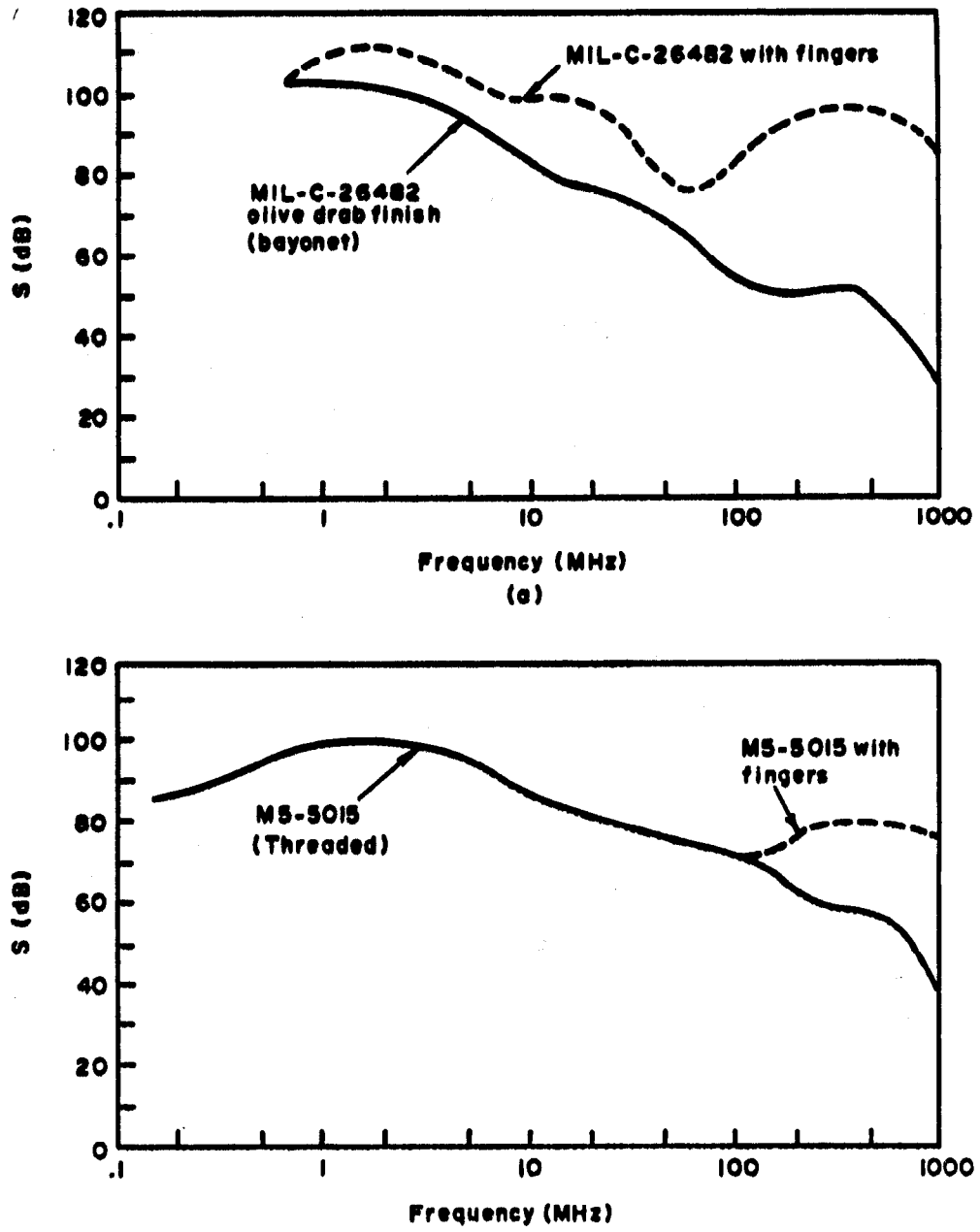

Figure 5-55. Effect of added spring fingers on shielding effectiveness. (Source: ref 5-16)